BRNO UNIVERSITY OF TECHNOLOGY
VYSOKÉ UČENÍ TECHNICKÉ V BRNĚ

FACULTY OF MECHANICAL ENGINEERING
FAKULTA STROJNÍHO INŽENÝRSTVÍ

INSTITUTE OF SOLID MECHANICS, MECHATRONICS AND BIOMECHANICS
ÚSTAV MECHANIKY TĚLES, MECHATRONIKY A BIOMECHANIKY

MODIFICATION OF NANOMANIPULATOR USED IN ELECTRON MICROSCOPE
ÚPRAVA NANOMANIPULÁTORU POUŽÍVANÉHO V ELEKTRONOVÉM MIKROSKOPU

MASTER'S THESIS
DIPLOMOVÁ PRÁCE

AUTHOR
AUTOR PRÁCE
Bc. Ondrej Habarka

SUPERVISOR
VEDOUCÍ PRÁCE
doc. Ing. Jiří Krejsa, Ph.D.

BRNO 2016

BRNO FACULTY OF MECHANICAL ENGINEERING
UNIVERSITY OF TECHNOLOGY

Master's Thesis Assignment

Institut:	Institute of Solid Mechanics, Mechatronics and Biomechanics
Student:	**Bc. Ondrej Habarka**
Degree programm:	Applied Sciences in Engineering
Branch:	Mechatronics
Supervisor:	**doc. Ing. Jiří Krejsa, Ph.D.**
Academic year:	2015/16

As provided for by the Act No. 111/98 Coll. on higher education institutions and the BUT Study and Examination Regulations, the director of the Institute hereby assigns the following topic of Master's Thesis:

Modification of nanomanipulator used in electron microscope

Brief description:

The aim of the thesis is in modification of nanomanipulator, that is used in electron microscope, in order to improve its behavior when performing the smallest motion steps. The selection of proper lubricant and stiffness of prestressed springs will probably be essential. The thesis is defined in cooperation with FEI Company.

Master's Thesis goals:

1. Analysis of natural frequencies based on the variable stiffness of prestressed springs in nanomanipulator mechanism.
2. Selection of proper lubricant and experimental verification of its influence on manipulator behavior, with respect to the requirements in semiconductor industry.
3. Proper setting of parameters in feedback control for modified manipulator.

Bibliography:

Robert Munnig SCHMIDT, Georg SCHITTER a Jan van EIJ: The design of high performance mechatronics, high-tech functionality by multidisciplinary system integration. Amsterdam: Delft University Press, 2011, 753 p. ISBN 978-160-7508-267.

Stuart T. SMITH.: Foundations of ultraprecision mechanism design. Repr. with corr. Yverdon, Switzerland: Gordon and Breach Science Pub, 1994. ISBN 978-288-4490-016.

Students are required to submit the thesis within the deadlines stated in the schedule of the academic year 2015/16.

In Brno, 20. 11. 2015

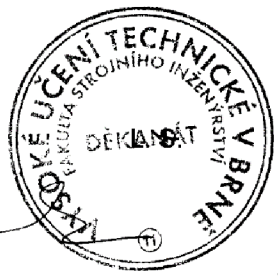

prof. Ing. Jindřich Petruška, CSc.
Director of the Institute

doc. Ing. Jaroslav Katolický, Ph.D.
FME Dean

Abstract

The goal of this master's thesis is to improve the smallest step performance of the nanomanipulator, that is used in electron microscope. The first part deals with analysis of the mechanism in order to find possible solutions. Further the thesis deals with testing the solutions such as optimizing stiffness of the pretension springs of the mechanism or changing lubrication of the worm drive of the mechanism.

Result of the thesis is choice of the most suitable solution according to tests results and then modification of the nanomanipulator.

Abstrakt

Cílem této diplomové práce je zlepšit chování nanomanipulátoru, používaného v elektronovém mikroskopu, při vykonávaní nejmenších kroků pohybu. První částí je analýza mechanismu za účelem nalezení možných řešení problému. Dále se práce zabývá testováním řešení jako je optimalizace tuhosti předepínacích pružin mechanismu anebo změna mazání šnekového převodu mechanismu.

Výsledkem práce je výběr nejvhodnějšího řešení problému na základě výsledků testů a následná modifikace nanomanipulátoru.

Key words

nanomanipulator, electron microscope, smallest step, worm drive, pretension springs

Klíčová slova

nanomanipulátor, elektrónový mikroskop, nejmenší krok, šnekový převod, předepínací pružiny

Bibliographic citation

HABARKA, O. *Úprava nanomanipulátoru používaného v elektronovém mikroskopu.* Brno: Vysoké učení technické v Brně, Fakulta strojního inženýrství, 2016. 53 s. Vedoucí diplomové práce doc. Ing. Jiří Krejsa, Ph.D..

DECLARATION

I declare, that I elaborated this master's thesis only by myself, under the supervision of doc. Ing. Jiří Krejsa, Ph.D. and with the use of literature and other sources, which are all quoted at the end of the thesis.

Brno 26.5.2016

.....

Bc. Ondrej Habarka

Thanks

I would like to thank to the FEI Company for giving me the opportunity to elaborate this thesis and to every colleague who helped me.

Then I would like to thank to my supervisor doc. Ing. Jiří Krejsa, Ph.D. for guiding and giving me many valuable advices.

Finally, I would like to thank to my family for support during studies.

CONTENTS

INTRODUCTION

Electron microscopy has a great use in many branches of industry and science. One of the branches in which it plays an important role is semiconductor industry. Together with continual progression in this field there is constant demand for better tools to help the development. Electron microscopes specialized for this work are often equipped with a nanomanipulator which is used for a material sample manipulation in a process of the sample preparation. The sample can be a thin lamella with thickness of a lot less than one micrometer. The process of preparation can even be a fully automated recipe with no human operator interference so it automatically requires confidently working tools.

This thesis deals with the nanomanipulator used in the electron microscope and was assigned with collaboration of the FEI Company. The main goal is to improve the performance of a smallest step while maintaining the other characteristics. Considering the complexity of the whole design only minor changes can be applied. Also the low cost of change is always highly appreciated.

The improvement could lead to better overall performance and increase the value of the nanomanipulator. Automated recipes could be performed with even more precision and success.

ISSUE OVERVIEW

The aim of this chapter is to find a solution to the issue. Starting with an introduction to electron microscopy, showing the difference between scanning and transmission electron microscope, explaining the purpose of the nanomanipulator with an example of its usage. Followed by the description of the nanomanipulator structure, its smallest step characteristics and the feedback control. After knowing the basic principles and understanding the mechanics it should be possible to predict what could be done to solve this engineering issue.

1.1. Electron microscope

Electron microscope uses charged particles (electrons) similarly like optical microscope uses visible light to enlarge an object. The difference is that optical microscope uses transparent lenses to focus light while electron microscope uses electromagnetic or electrostatic lenses to focus electron beam. The resolution is limited for both principles because of wavelength. Light enables typical magnification of 1000 times but electrons enable 4 million times magnification compared to the bare human eye. In other way of saying it means resolution less than 0.05 nm which means the ability to see individual atoms. [1]

Figure 1: FEI Scios Dualbeam electron microscope. [2]

There are two basic types – scanning electron microscope (SEM) and transmission electron microscope (TEM). SEM uses narrowly focused electron beam scanning an object in raster pattern. At every point of the pattern it senses the secondary or the backscattered electrons witch carry some information of the object surface, step-by-step building an image after some computer processing. TEM principle is more similar to optical microscope. The focused electron beam passes through a thin sample interacting with it and then is projected on the fluorescent screen which emits visible light observed by a human operator. The sample has to be very thin in order to be able for the beam to pass through. [1]

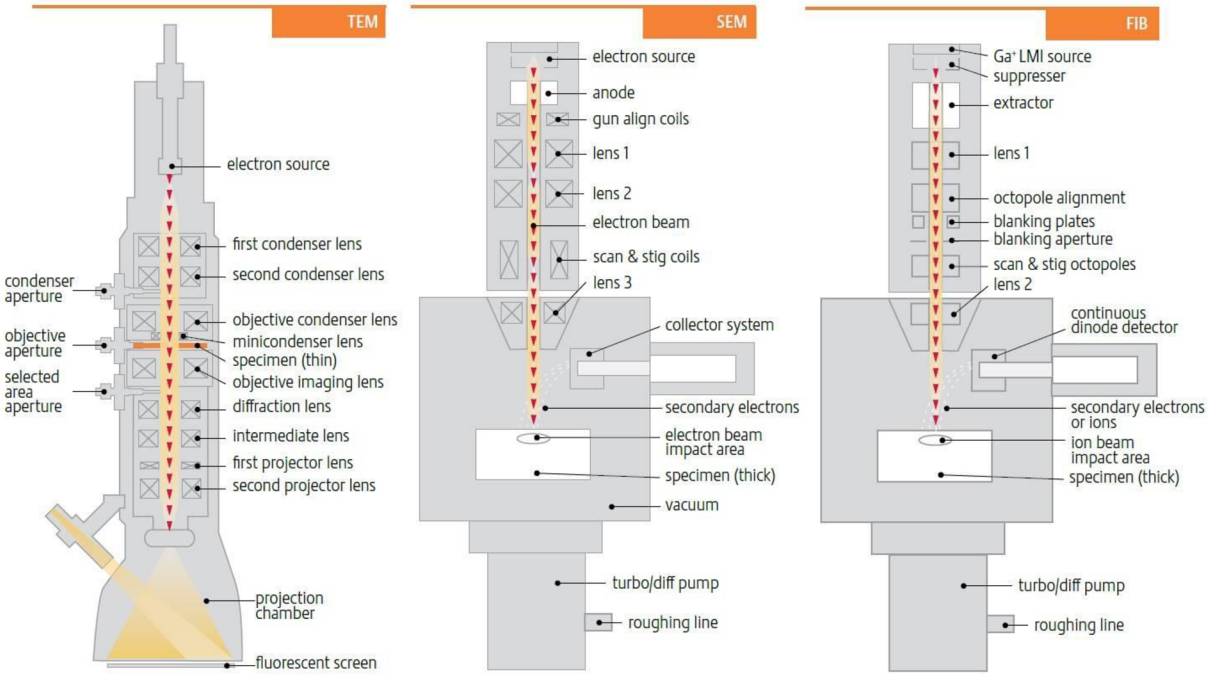

Figure 2: Comparison of SEM with TEM and FIB. [1]

Another type of microscope is a focused ion beam microscope (FIB) working similarly to SEM but electrons are replaced by ions, usually positively charged gallium. Thanks to much higher mass of ions, the FIB is not only able to scan but also, when targeted to defined area for some amount of time, to precisely remove material from the sample. [1]

FIB can be added to SEM positioned in the way that both beams are focused on one point on the sample. In Figure 1 we can see the so called DualBeam microscope with vertical electron column placed above the chamber combined with FIB column on the upper left side of the chamber. There is also the nanomanipulator placed in the upper front side of the chamber,

described in to following subhead. With this technology it is possible to see in real time how the material is removed by ions what can be used for sample modification. [1]

1.2. The nanomanipulator

Only watching may be enough for many scientific experiments but sometimes there is a need to physically move things. That can be a problem at nanoscale because for this work there are not many tools available. The nanomanipulator described here is one of the few.

1.2.1. The role of the nanomanipulator in the electron microscope

The nanomanipulator can be used to lift a piece of material cut from the bulk material and transfer it to a standard TEM grid that can be afterwards loaded into TEM. In semiconductor industry it is usually a sample in shape of thin lamella called TEM lamellae. Using the backside thinning technique it can create an ultra-thin lamella, for example a cross section of transistor. This kind of analysis can be a part of manufacturing process monitoring. One of the key benefits of the nanomanipulator is the possibility of automation of the whole preparation process. Sample preparation quality is then not affected by the skill of an operator but requires high precision and repeatability of the manipulator movement. [1] [3]

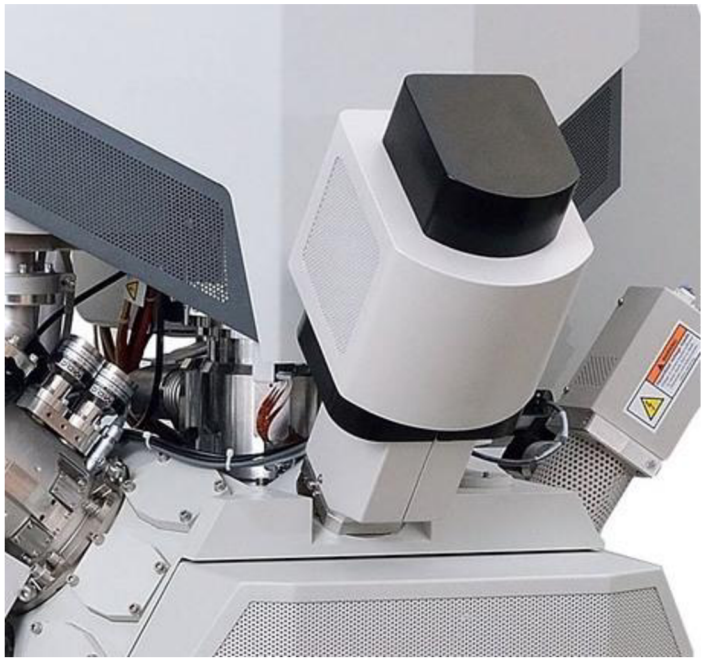

Figure 3: The nanomanipulator. [2]

1.2.2. TEM lamellae preparation

In the manufacturing process monitoring, SEM can be used to create a cross section image of an electronic device. When the SEM resolution is not sufficient, the TEM lamellae can be created and observed in TEM. It can be done by hand polishing in the lab or by a DualBeam (FIB/SEM) system. An example of the whole flow is shown in the Figure 4. [4]

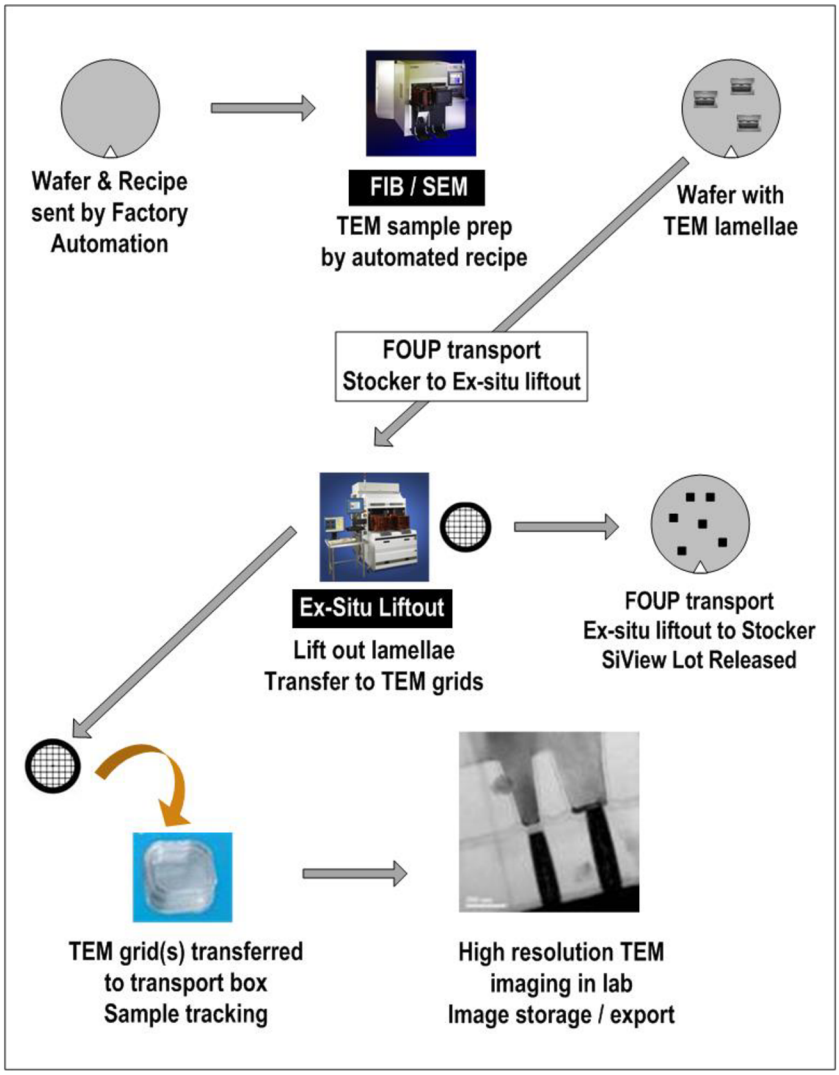

Figure 4: TEM sample preparation flow. [4]

The part of the flow where the nanomanipulator is involved is the process of cutting the TEM lamellae from the bulk material. A stage is in several steps tilted in the way that the FIB can mill two rectangular holes next to each other in order to create a lamella between them, undercut the lamella and uniform its thickness. Before the lamella is fully separated from the bulk material, the needle of the nanomanipulator approaches close to an edge of the lamella. Then the lamella is attached to the tip of the needle using a material deposition. Finally a last

cut is performed that detaches the lamella from the bulk material, so it can be lifted out and transferred to the TEM grid. A similar process is applied to attach the sample to the grid and detach it from the needle. [3] [4]

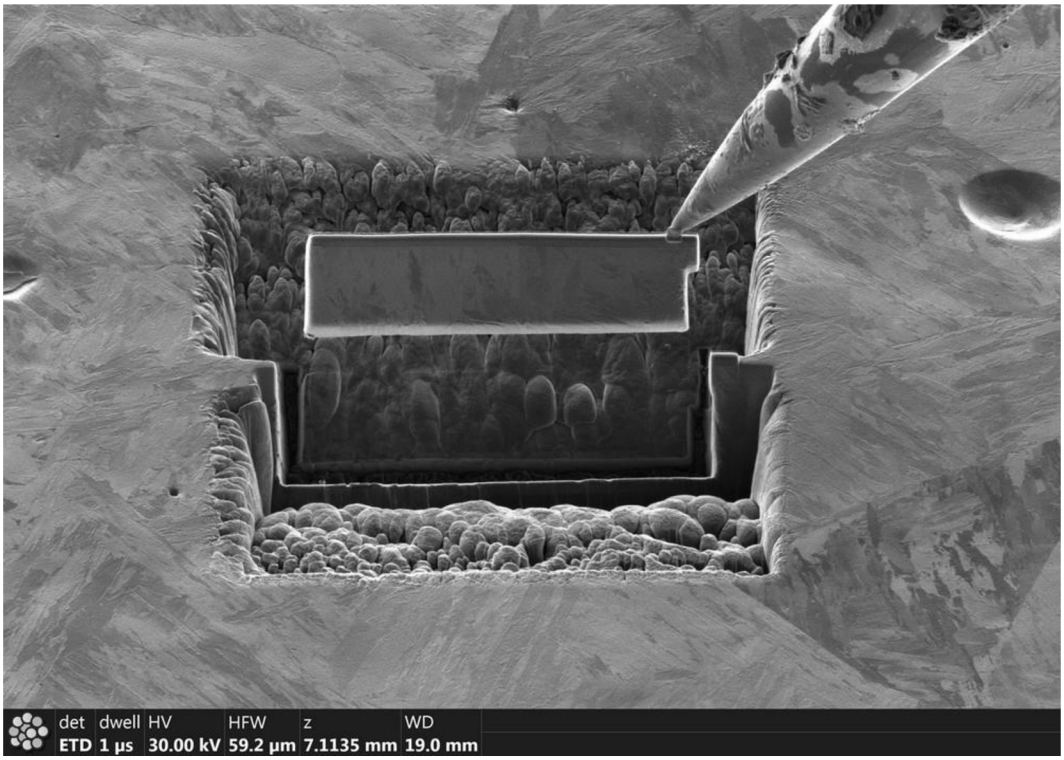

Figure 5: TEM lamellae lift-out with the needle of the nanomanipulator. [5]

1.2.3. How does it work?

The nanomanipulator is fully functional and operating device, designed several years ago. None of the design work was part of this thesis. The aim of this thesis is only to do some additional changes to already functional device. How does this device work is described on the following pages.

As mentioned before, the nanomanipulator has no tweezers or a fingers mechanism at the end of an arm to hold samples, it only uses a sharp needle. Tip of the needle is capable of movements in X, Y and Z axes of the relative coordinate system linked to the coordinate system of the microscope. The absolute range of all axes is 1 mm. To access different points of larger object we can move whole object with the stage on which it is mounted.

There is no need for improving Z axis performance so this thesis deals with X and Y axes only. The X and Y axes have the same working principle. The kinematic scheme is shown in the Figure 6.

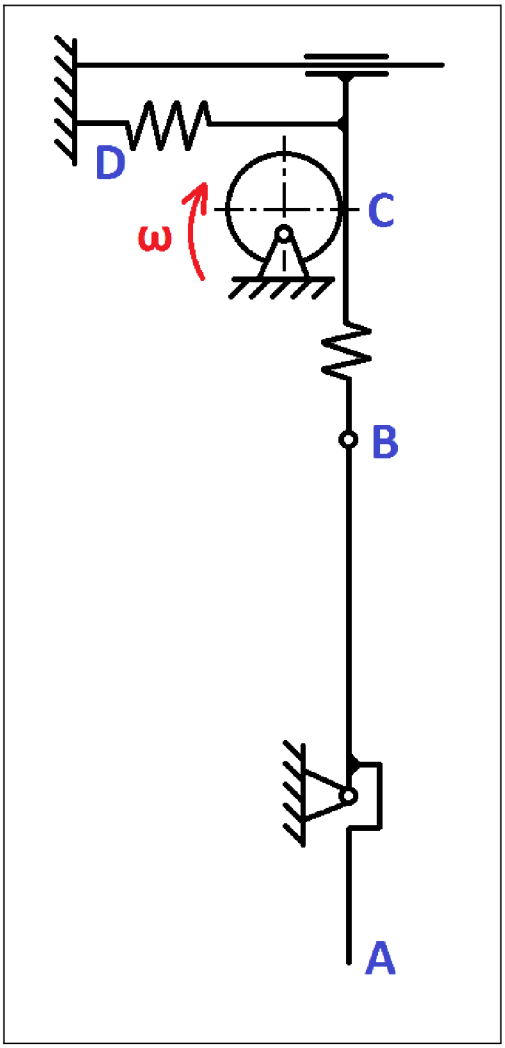

Figure 6: Kinematic scheme of X/Y axis

The arm of the nanomanipulator is the rod between the points A and B in the scheme, called shaft, with length of 500 mm. It has a pivot point in the third of its length in order to make the shaft act as a lever. The tip of needle is at the point A, the other side of the shaft is linked to a carriage via special flexible shaft coupling. The coupling is the link between linear movement of the carriage and rotational movement of the shaft, what works for small displacements. Thanks to the lever effect, needle displacement equals haft the carriage displacement, what increases accuracy.

The carriage is displaced by movement of a ball bearing on an eccentric cam (point C in the scheme). The eccentric cam simply pushes against the carriage. There is also an extension

spring (point D) pulling the carriage against the cam to maintain the contact between them. The extension spring is important because it pre-loads the mechanism and eliminates any backlash. The eccentric cam is driven by a DC motor coupled with a worm drive, see Figure 7. The worm drive has gear ratio of 40:1. The DC motor does not have additional gearbox.

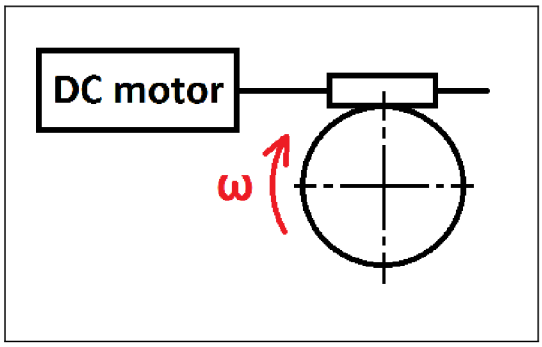

Figure 7: The worm drive scheme

Note that angular velocity ω is the same for both kinematic schemes in Figure 6 and Figure 7 because the worm gear and the eccentric cam are on the same shaft, see Figure 8 below.

Figure 8: Eccentric cam shaft with worm gear

It is important to realize how does the extension spring eliminate any backlash. The eccentric cam is always pre-loaded by the spring, what creates a constant moment applied on the worm drive. The eccentric cam never makes full rotation around its axis, it is rotated for only approximately ±60 degrees from the middle position as showed on the scheme. The eccentricity of the cam is 1.4 mm. The pre-load also eliminates any radial play in ball bearings. There are also some wave springs in the worm drive gearbox to eliminate the axial play in the bearings.

Position of the nanomanipulator is measured by a linear incremental encoder mounted on the carriage. Actual position of the tip of needle is than simply calculated according to the

lever ratio of the shaft. As mentioned before, movement of the needle is half the movement of the carriage.

The nanomanipulator is mounted on a microscope chamber. Needle is pointing inside to the middle of the chamber. Mechanism with the DC motors is outside the chamber. Therefore the design must deal with vacuum on one side and atmospheric pressure on the other side of the nanomanipulator.

Since the nanomanipulator is mounted tilted on the chamber, there is a gravity isuue. Gravity of the mechanism is pulling against the pretension spring in the vertical X axis what decreases the total pretension force. The Y axis is horizontal therefore gravity does not play a role here. That applies for a standard mounting position of the nanomanipulator however there are other different mounting positions possible. Then the gravity issue applies for the both axes.

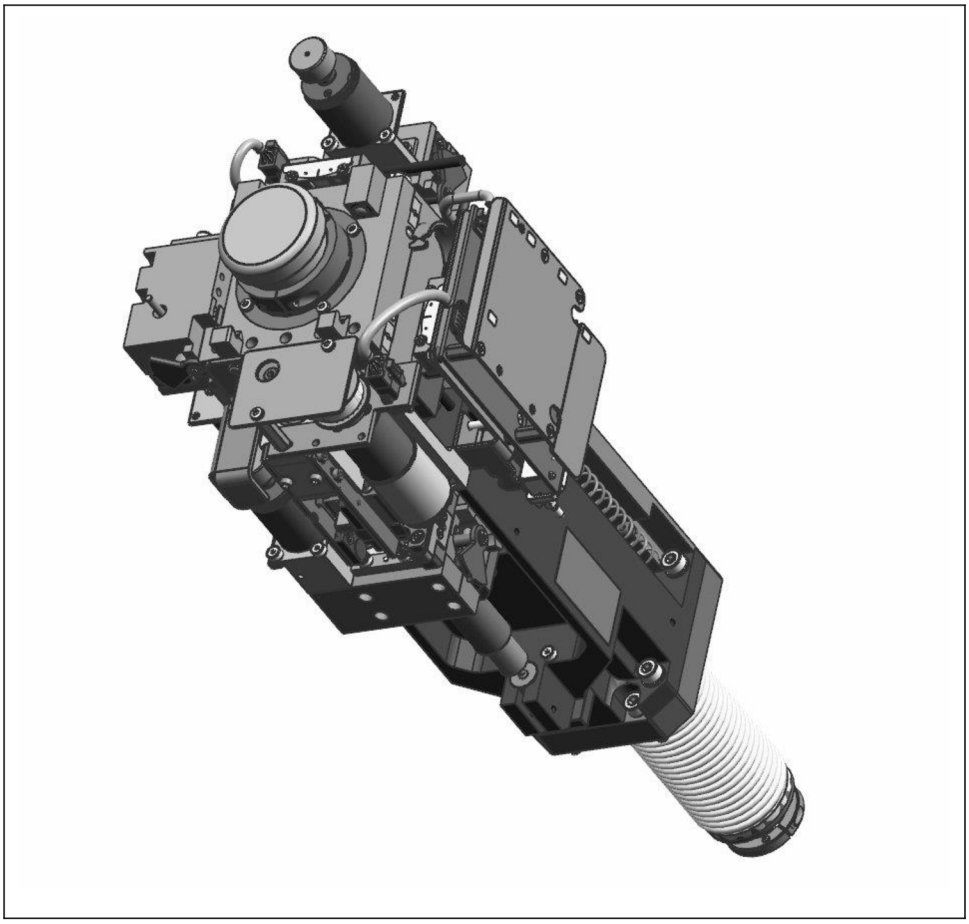

Figure 9: The nanomanipulator assembly [6]

Figure 9 shows the complexity of the whole device. Therefore should be carefully considered what parts could and should be modified. After knowing the working principle it is possible to name the key parts of the X and Y axes mechanisms. It is the shaft, the carriage, the

eccentric cam and its ball bearing, the worm drive and the bearings of the gearbox, the extension spring and the DC motor. All bearings are very precise, made by time-proven manufacturer, so there is unlikely some space for improvements. The same can be said about the DC motor. On the other hand the worm drive and tension of the extension spring appear to be the key factor. Because there is a friction between worm and worm gear in the worm drive, the lubrication could have great influence on smoothness of movement. How much is the gear loaded depends on tension of the extension spring, which could also have such influence. Also changing the gear ratio of the worm drive should influence behavior of the mechanism.

1.1.Feedback control

PID feedback controller controls the nanomanipulator when it is performing a small steps. In feedback control the position of the motion system is monitored by an encoder and the controller generates a control action based on the difference between desired and actual position. The feedback loop is closed based on information from a sensor. Big advantage of feedback controlled systems is that stability and performance requirements are guaranteed even for parameter variations of the controlled mechatronic system. On the other hand it has limited reaction speed because it reacts on difference between the desired and the measured position what means that the error has to occur before the controller can eliminate it. [7] [8]

The controller must be tuned according to dynamic properties of the motion system. The dynamic properties are experimentally investigated by applying external forces to the system and simultaneously measuring the response of the system to this stimulus. The response to the stimulus with wide frequency spectrum that is continuously available is called frequency response. This kind of dynamic properties investigation is used for the nanomanipulator. [7]

There are two graphical representations frequently used to display the response of a dynamic system. The Bode plot and the Nyquist plot. [7]

1.1.1. Bode plot

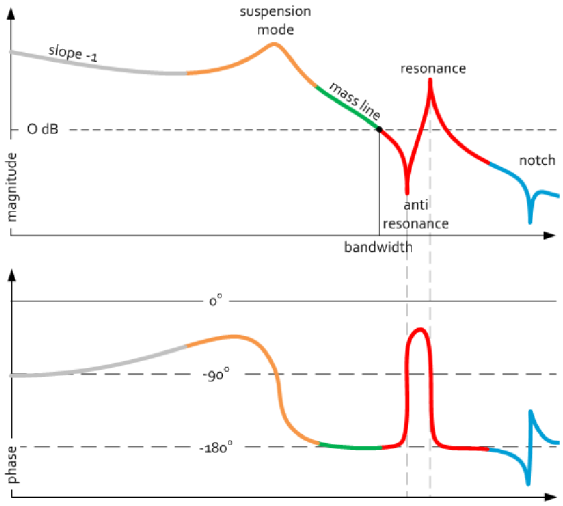

Figure 10: Example Bode plot of a motion system [9]

The Bode plot shows the magnitude and phase response upon a continuous frequency stimulus as function of frequency. It consists of two graphs, one above the other, with the same horizontal axis with frequency as parameter. The upper graph shows the ratio between the magnitude of the response and the magnitude of the stimulus on the vertical axis. The other graph shows the phase shift on the vertical axis relative to phase of the stimulus. The Bode plot shows the response of the system when all frequencies are continuously present at the stimulus. Both frequency and magnitude scales are logarithmic to base 10. [7] [10]

1.1.2. Nyquist plot

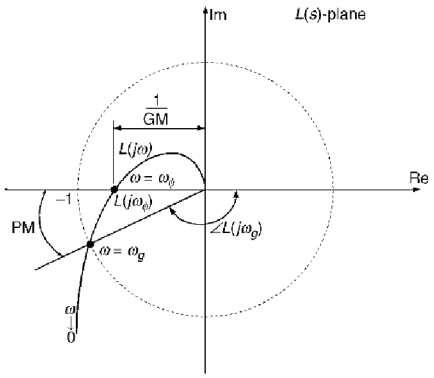

Figure 11: Nyquist plot example [10]

The Nyquist plot shows the magnitude and phase response on continuous frequency stimulus as function of frequency but only in one graph. It is a polar coordinated two dimensional vector plot where magnitude is represented by length of vector starting in the origin

and ending in a point on a curve. The phase is represented by the angle of vector relative to the positive horizontal axis. There is one vector for each frequency from a frequency spectrum. When these vector are connected, the curve is obtained with the frequency as parameter along the curve. The curve represents the response as function of increasing frequency in the direction of the origin. This plot is often used for the stability and robustness analysis of feedback controlled systems. [7] [10]

1.1.3. Control design

The dynamic properties of the nanomanipulator are investigated by running automated recipe called the Xfer test. A noise signal containg a variety of frequencies is the input to the DC motor during the test. The DC motor then acts as the stimulus and the actual position is measured simultaneously. Result of the test is the frequency response of the nanomanipulator depicted by the Bode, Nyquist and sensitivity plot as shown in the Figure 12. There is a set of specified margins in the curves of the plots which must lay below or above defined values. For example a maximum sensitivity is found in the sensitivity plot and this point must lay below a maximum allowed value. Further explanation of the diagrams analysis is out of the scope of this thesis.

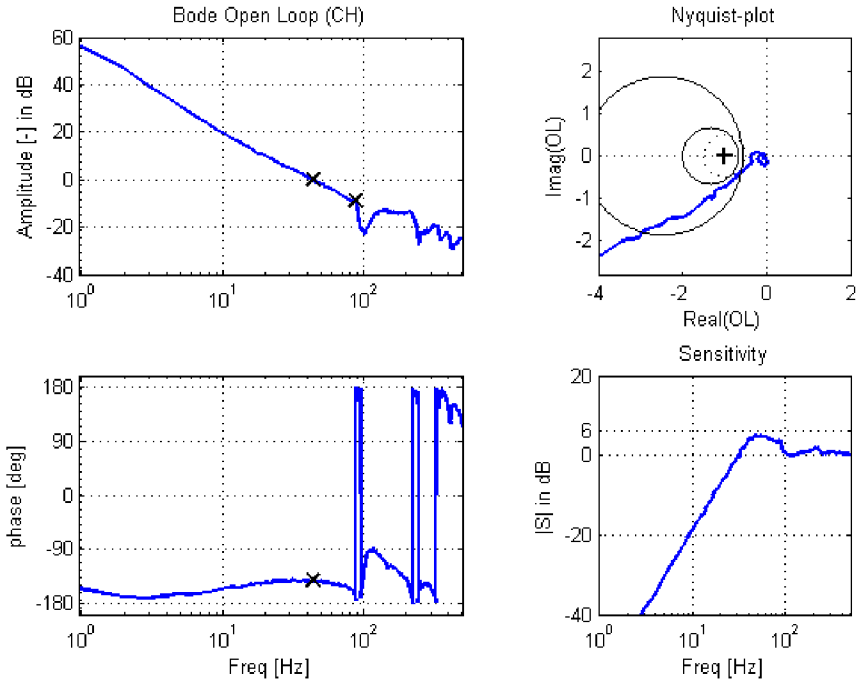

Figure 12: Xfer test for the X axis [11]

There is an application called the Control design developed by FEI which is used for tuning the controller of the nanomanipulator. A measured data from the Xfer test can be opened in the application which shows all the diagrams mentioned before. There is a load of parameter settings which define the controller behavior, placed on the right panel of the user interface, see the Figure 13. A change of any parameter is instantly translated in a change of the diagrams what makes the tuning much easier. The most critical are settings of PID parameters but also settings of the filters eliminating magnitude rise in a resonance and the filters eliminating eventual notches. The margins can be also shown which allows checking whether the tuning meets the requirements.

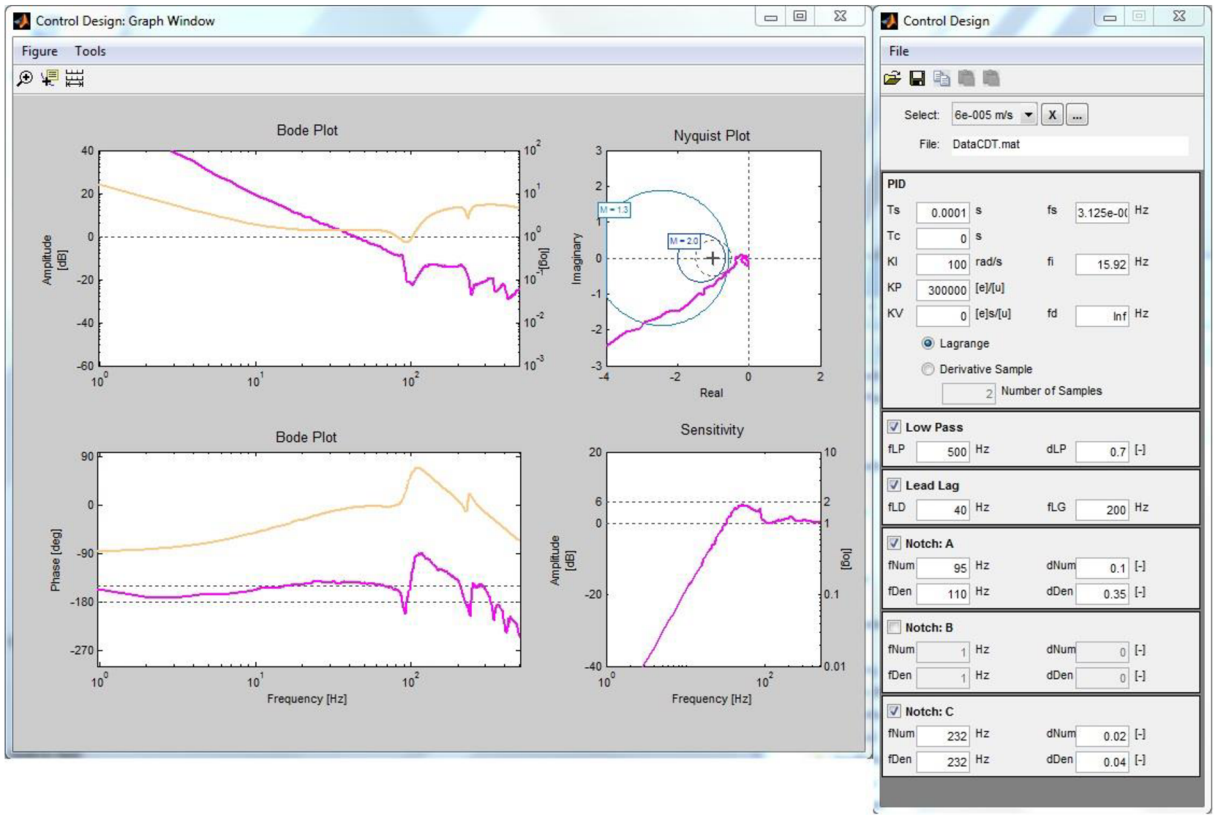

Figure 13: Control design application [11]

1.2. The smallest step

For the reason that some data in this thesis may be confidential, the smallest step length will be defined as the constant a which value is not stated. Some value had been chosen for the tests and will be the same for all tests stated in this thesis. Note this value is less than one micrometer. Value 1 a is the desired step length. For example if a measured step length is 1.5 a that means the step was 1.5 times bigger than the desired step. The position will be also measured in step length a. From now on, this constant represents new unit of length. This allows comparison of results without showing confidential data.

1.2.1. Requirements for the mechanism

To illustrate the required level of precision of the DC motor and in fact the whole mechanism movement, there is a simple calculation of how small angle of rotation must the DC motor perform to make a small step. In this calculation the 1 μm step of the nanomanipulator (the tip of its needle) will be considered. Step of the carriage it twice the nanomanipulator step because of the lever ratio of the shaft. Then the rotation angle of the eccentric cam is calculated from its eccentricity. The worm drive then multiplies the angle by 40, according to the gear ratio.

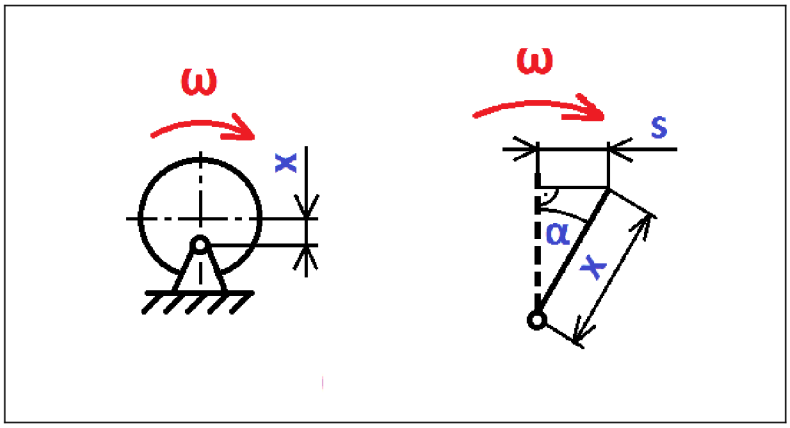

Figure 14: Sketch for calculation of the eccentric cam angle.

$$s = l \cdot r = 0.001\ mm \cdot 2 = 0.002\ mm$$

Where l is length of the nanomanipulator step, s is length of the carriage step and r is the lever ratio of the shaft.

$$\sin \alpha = \frac{s}{x}$$

Where α is an angle of rotation of the eccentric cam and x is the eccentricity, 1.4mm.

$$\alpha = \arcsin\left(\frac{s}{x}\right) = arcsin\left(\frac{0.002\ mm}{1.4\ mm}\right) = 0.0819°$$

$$\alpha_m = \alpha \cdot i = 0.0819° \cdot 40 = 3.27°$$

Where α_m is angle of rotation of the DC motor and i is the gear ratio of the worm drive.

We can see that even when the step is relatively big, shaft of the DC motor rotates by angle of only few degrees. Note that step could be many times smaller. Similarly the smoothness of the gearbox running must be high since the gear rotates by angle of only fraction of degree. Also the motor controller operation must be very precise.

1.2.2. Motion of the smallest step

The nanomanipulator motion is controlled by the NYCe 4000 motion control system with integrated drive technology, manufactured by Bosch Rexroth Company. It supports wide range of motors and encoders. The nanomanipulator has brushed DC motors and linear incremental encoders. NYCe 4000 consists of motion control unit, drive unit and software running on standard industrial PC. Software in the PC is called host software and consists of a number of subsystems. The whole software architecture is complex, therefore is not described in detail. For more information see the referenced documents. [12]

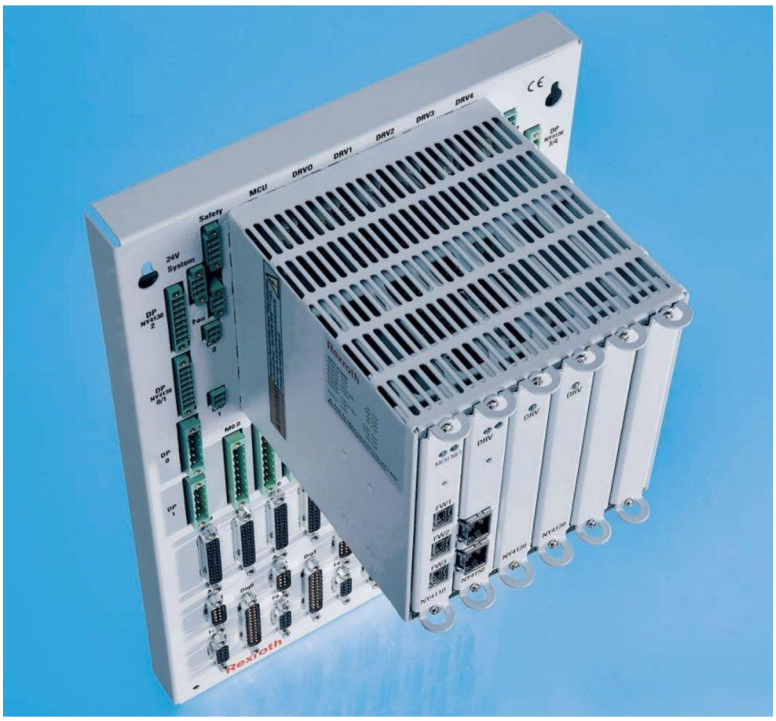

Figure 15: NYCe 4000 motion control unit. [13]

One of the software subsystems, the Single Axis Control (SAC) subsystem provide functionality to control and monitor axes in a motion system. Each axis is controlled independently from each other. Controlling means generating a setpoint position and forcing the actual position to the setpoint position. [12]

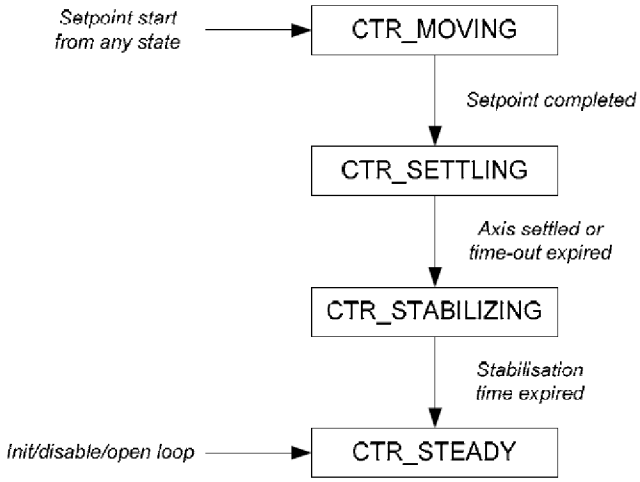

Figure 16: States for controller stabilization. [12]

While the nanomanipulator is moving, the controller of an axis is going through 4 states. Moving, settling, stabilizing and steady state, see Figure 16 and Figure 17. First the trajectory is planned between an initial and a setpoint position. Settling state starts at the end of that trajectory regardless of the actual motor position. During settling state, the program waits for the actual motor position to be within a settling window for at least certain amount of time. Some additional time for stabilization is added in the stabilizing state, right before steady state.

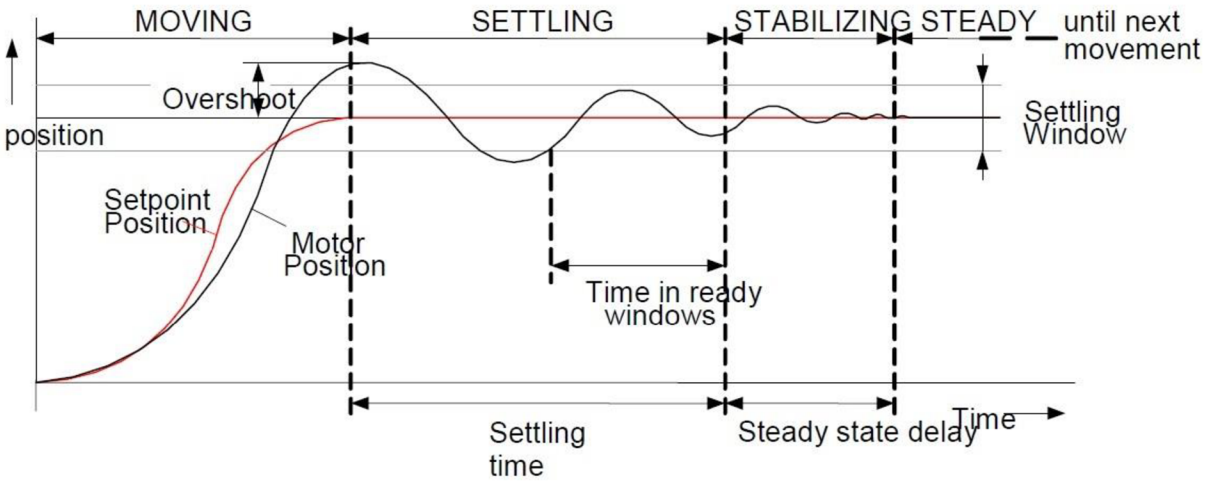

Figure 17: States for controller with respect to position. [12]

The transitions between the states are determined by the settings of the parameters:

- SAC_PAR_POS_READY_WIN
- SAC_PAR_VEL_READY_WIN
- SAC_PAR_TIME_IN_READY_WINDOWS
- SAC_PAR_STEADY_STATE_DELAY

These parameters define the settling window – how precise position together with how maximum velocity of settling should be reached within the settling state. Also the maximum length of the states is defined. [12] [14]

When performing the smallest step, actual motor position figure looks different from the Figure 17. It is because of very low speed and torque of the motor in this case. After a setpoint is generated according to a step length and an initial position, controller begins to slowly rise voltage on the motor until it starts to move. Rise of the voltage is slow because the setpoint position is very close to the initial position. There is a static friction present in the gearbox, therefore the motor starts to move at a certain voltage. Very soon after it starts to move, the setpoint position is achieved due to small step length. Voltage begins to fall and very soon the torque is too small to overcome friction and the movement stops. See Figure 18. Meanwhile the time in ready windows is counted since the setpoint position is achieved. At the end of that window, voltage drops to zero and the step is finished.

Immediate voltage drop causes the motor to revolve a little bit in opposite direction, making a back step, what can be also seen at Figure 18. Size of the back step directly depends on the voltage amplitude.

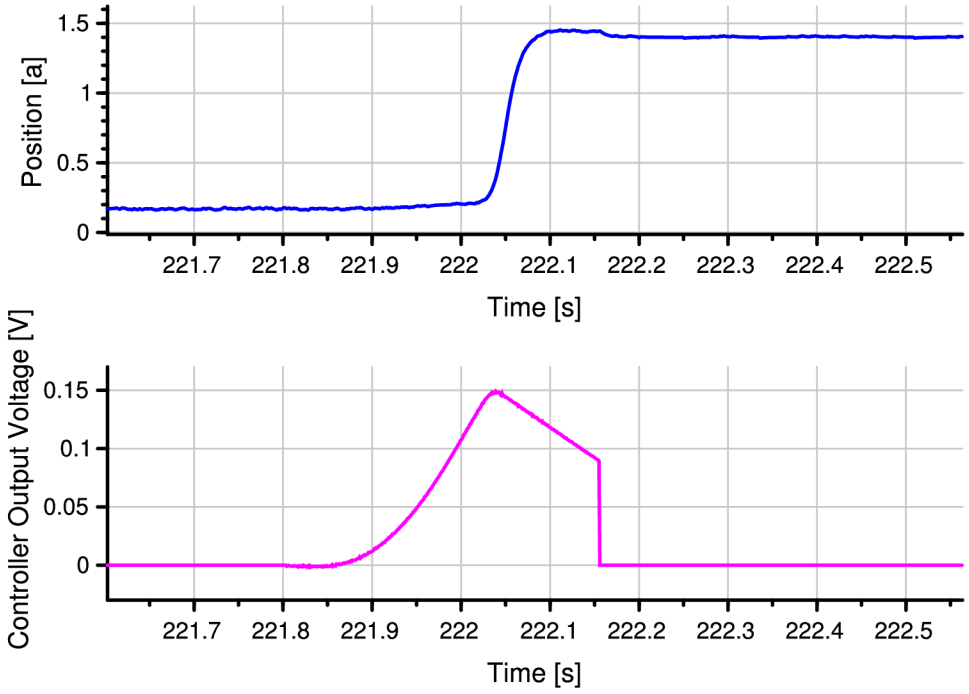

Figure 18: Position and Controller output voltage during the smallest step

A movement of the nanomanipulator typically take place in the moving state. However when performing the smallest step, the planed trajectory is so short that the moving state ends too soon. The movement than take place in the settling state.

1.2.3. Test procedure

There are several test routines to verify performance of every new nanomanipulator. These tests were designed together with the design of the nanomanipulator and this design work was not part of this thesis. Test routines important for the smallest step testing are described in this and the following subhead.

The most valuable is the smallest step test. A set of 20 steps is performed in one direction followed by another 20 steps in opposite direction, see Figure 18.

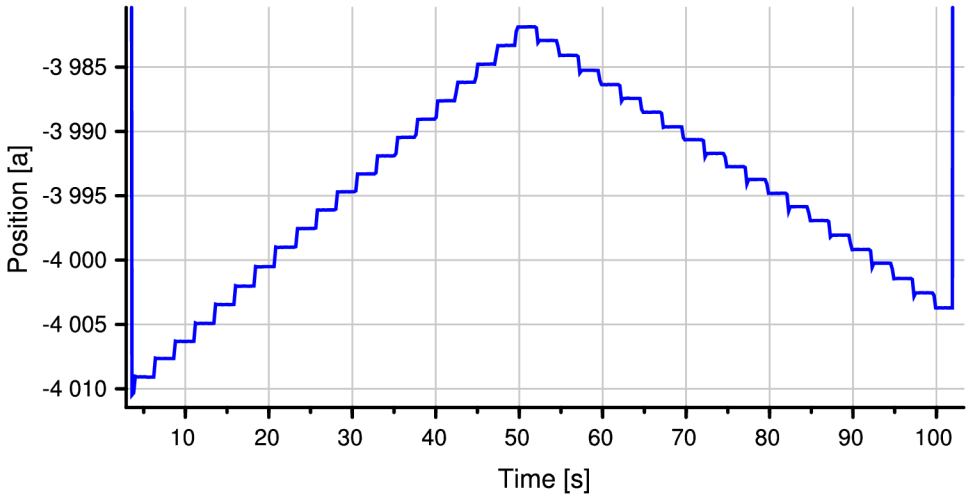

Figure 19: First set of steps during test procedure

This set is repeated 5 times at various positions across the range of the nanomanipulator, see Figure 19. Note that the smallest steps are too small to be visible at this figure. The figure shows how the sets of these steps are performed only. The test routine is performed for both axis independently.

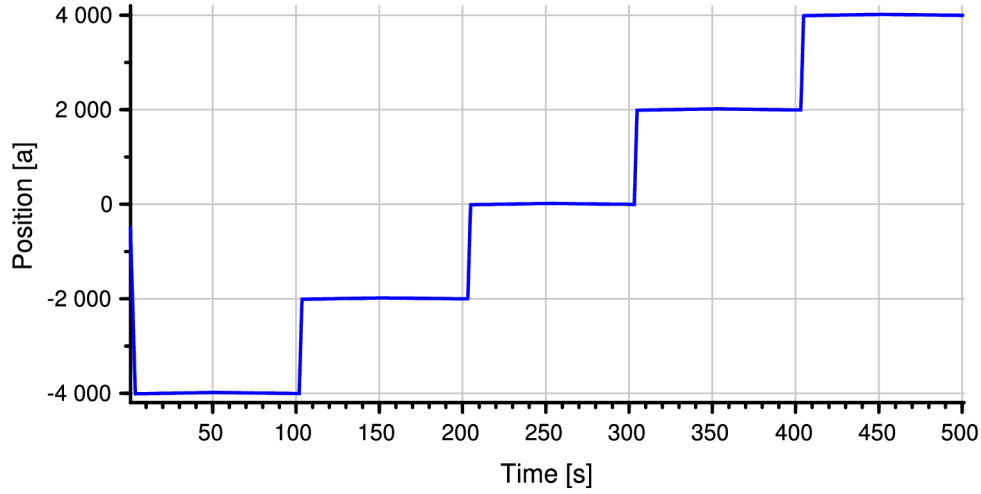

Figure 20: Test procedure

Result of the whole smallest step test is a table with values of an average step length and standard deviation of steps calculated from each set of steps, see Table 1. Average step length should be close to the desired step length, $1a$ in this case. Standard deviation describes the variability of steps length within the set and should be as low as possible. From the values it is possible to determine whether a nanomanipulator meets the standards. In this thesis they will be used as reference to compare current performance with results.

Move test is designed to check how smooth the mechanism movement is. The mechanism performs a move through the whole range in one and then in opposite direction for both axis independently. The motor is controlled to a constant speed. Controller output voltage is measured while a speed of motor is constant. The values should lie within a desired range.

1.2.4. Current performance

Current performance measurement will produce a data that will help to better understand the issue and will also serve as a reference for results evaluation. Previously described test routines will be performed for both axes. Starting with the move test in the Figure 21.

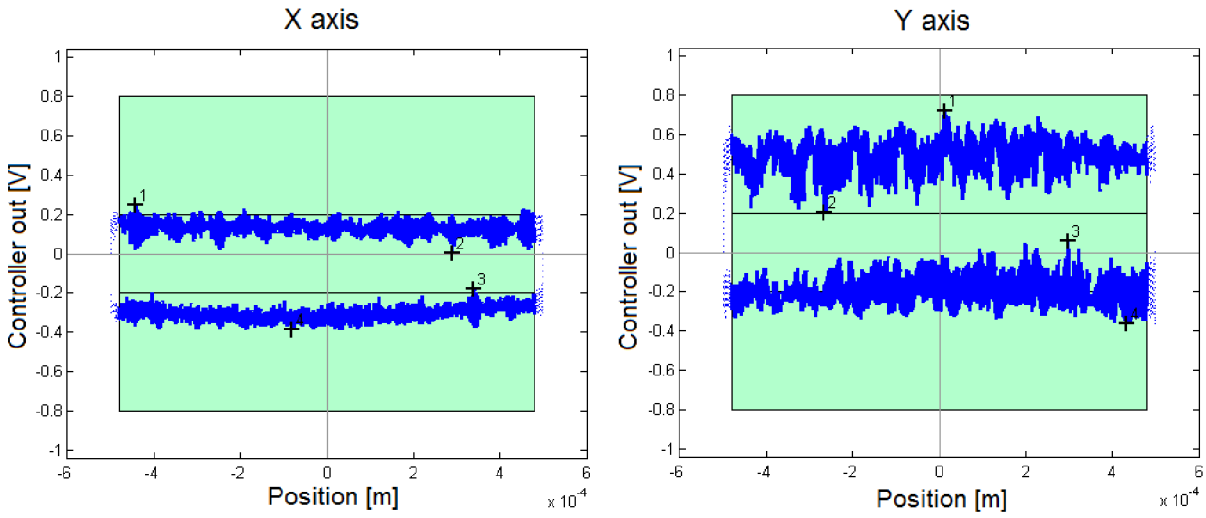

Figure 21: Move test [11]

The move test shows smooth operation of X axis where we can see only little instability. However the higher controller output voltage in Y axis means there is more torque needed for the movement in one direction. It is positive direction in which means against the direction of the pretension force. Lower voltage in X axis could be explained by the presence of force exerted by gravity of the nanomanipulator, pulling against the pretension spring lowering the total pretension force. The gravity issue was described in subhead 1.2.3, in more detail.

The smallest step test was performed for both axes. A sample of typical performance during the test is shown in the Figure 22. For X axis a step length in positive direction is a bit bigger than desired $1a$ and we can also see significant back step in negative direction. Similar deviations are present in the Y axis figure but for opposite direction.

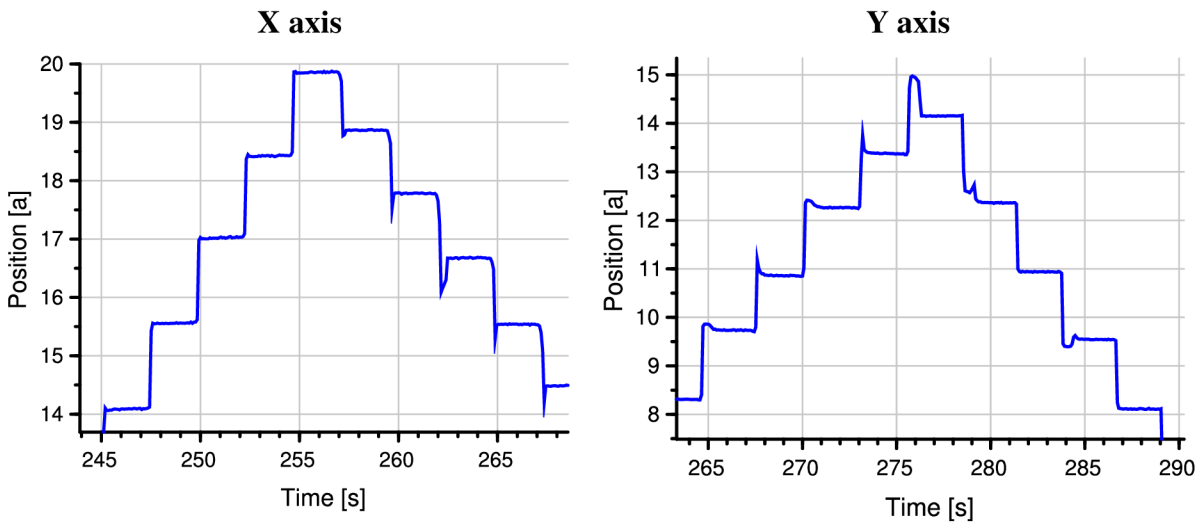

Figure 22: Typical smallest steps of X and Y axes

Complete results of the smallest step test are shown in the Table 1. The first column is a position of a set of steps. Values in the column "Average" confirm the different step length in relation to move direction. Low standard deviation values in the fourth column show that the step length is rather constant within a set of steps. That means there are no failures to perform a step at all, or at least the failures are rare.

X axis				Y axis			
Position [a]	**Direction**	**Average [a]**	**Standard deviation [a]**	**Position [a]**	**Direction**	**Average [a]**	**Standard deviation [a]**
-4,00E+03	Positive	1,422	5,36E-02	-4,00E+03	Positive	0,352	5,36E-02
-4,00E+03	Negative	1,092	5,54E-02	-4,00E+03	Negative	1,360	1,33E-01
-2,00E+03	Positive	1,422	1,08E-01	-2,00E+03	Positive	0,422	1,13E-01
-2,00E+03	Negative	0,942	8,84E-02	-2,00E+03	Negative	1,382	1,43E-01
0,00E+00	Positive	1,396	5,46E-02	0,00E+00	Positive	0,362	5,44E-02
0,00E+00	Negative	1,026	5,80E-02	0,00E+00	Negative	1,468	1,12E-01
2,00E+03	Positive	1,408	4,26E-02	2,00E+03	Positive	0,324	1,22E-01
2,00E+03	Negative	1,164	5,50E-02	2,00E+03	Negative	1,398	2,22E-01
4,00E+03	Positive	1,396	3,84E-02	4,00E+03	Positive	0,890	1,45E-01
4,00E+03	Negative	1,098	6,02E-02	4,00E+03	Negative	1,406	1,08E-01

Table 1: Current smallest step test results

The Xfer test was also performed for both axes. Results for the X axis are depicted in the Figure 12. Results for the Y axis are very similar therefore not stated. The Xfer test confirms good dynamic properties of the system. For this thesis it is intended for verifying that any physical changes on the mechanism did not affected the dynamics of the nanomanipulator.

1.3.Possible solutions

After considering everything stated in this chapter and other things, several possible solutions had been found. As a reminder it is important to mention that any change of the mechanism should be minor because of the design complexity and change cost. The lubrication of the worm drive could be analyzed since it could play a great role in smoothness of the drive running. Optimizing stiffness of the pretension springs is the second solution since the pretension force has direct impact on the performance as explained in previous subhead. Increasing the worm drive ratio could also have an effect because it would enlarge that extremely small angle of rotation of the DC motor when performing the smallest step.

GOALS DEFINITION

The aim of the thesis is in modification of nanomanipulator, that is used in electron microscope, in order to improve its behavior when performing the smallest motion steps. The thesis is defined in cooperation with FEI Company. The aim is to increase precision and steadiness of the smallest step. The design of the nanomanipulator and of the test recipes was not part of this thesis. Only a minor change is preferred because of complexity of the design and the change cost.

At first a lubrication of the worm drive will be analyzed since it could play a great role in smoothness of the drive running. Testing of various greases or oils will be performed. The move test and the smallest step test for each greasing will be performed. Results will be analyzed in order to create a comparison of lubricants in relation to the smallest step performance of each lubrication. Aim is to find a better lubrication than the currently used Braycote grease. A modification would be applied only if a lot better results would be achieved than with the Braycote grease.

Since the pretension force applied to the carriage of the mechanism has direct impact on the performance, stiffness of the pretension springs will be optimized. A set of springs with various stiffness will be tested. The smallest step test will be performed in order to compare them. If the tests will be successful, an optimal pretension spring will be calculated for each axis, considering various mounting positions of the nanomanipulator. Both axes currently have the pretension spring of the same stiffness. An optimal pretension spring with different stiffness for each axis will be calculated if the tests prove an advantage of such configuration while also considering various mounting positions of the nanomanipulator.

Testing of the worm drive with increased gear ratio will be performed because it would enlarge that extremely small angle of rotation of the DC motor when performing the smallest step, which could also have an effect on the smallest performance. The gear ratio will be two times higher than currently used 40:1 which means 80:1. Increasing the worm drive ratio will decrease size of teeth of the gear what will decrease durability of the worm drive. This modification would be therefore applicable only if the pretension sprigs stiffness would be significantly reduced.

Proper setting of the feedback control parameters will be done after modification of the nanomanipulator. The aim is to compensate system dynamics via control to achieve the same performance in terms of frequency response as before the modification.

After suggesting a modification it is necessary to check reliability before the modification is applied to the product. That will be done by performing tests on a great number of new systems. The aim is to assure a modification is relevant and to prove its steadiness. On the other hand it is also important to avoid any unwanted side effects which could be brought by the modification.

TESTING

A great number of tests had been performed in total. It started with testing of lubrication of the worm drive because it may have a great impact on the mechanism behavior and it could be started immediately without waiting for suppliers. Followed by pretension spring optimization and meanwhile testing of increased worm drive gear ratio.

1.4. Lubrication of the worm drive

A great variety of lubrications have been tested. From transmission oils with lower viscosity to greases with high viscosity and also with no lubrication at all. The list of all tested lubricants is stated in the Table 2.

#	**Lubrication**
1	Braycote Micronic 1613 Vacuum Grease
2	FeinOl
3	Molykote BR 2 Plus
4	Mogul LV 2-3
5	Mogul LV 2-3 (film)
6	no lubrication (without warmup)
7	no lubrication
8	Dry Lube
9	Braycote (2.measurement)
10	Renolit FLM 2
11	Promicron LED 2T

Table 2: Tested lubricants

All lubrications were tested for both axes. Before each test the mechanism was carefully disassembled. The worm drive was cleaned with isopropyl alcohol to dispose any remains of a previous lubricant. It was done with dust free wipes and dust free sharp swabs, cleaning gears tooth by tooth. Amount of newly applied lubrication was rather small but evenly distributed as it was advised by experienced FEI technicians. The whole procedure was done in a clean room environment to avoid any dust particles to contaminate lubrication of the worm drive.

A warmup automated recipe was performed after applying each lubrication before any tests. It was intended for the gears to better mesh with each other together with a lubrication. The recipe consisted of one hundred moves across the range of the nanomanipulator and back,

for both axes simultaneously. The warmup recipe takes approximately one hour due to slow movement speed.

The Braycote grease is currently used in the worm drive. It is vacuum grease based on Teflon particles. However the worm drive is not exposed to vacuum therefore the lubrication does not have to be vacuum suitable. Other tested lubricants are designed for various branches of industry for example graphite based Renolit is designed for heavy machinery of FeinOl and Dry Lube are bicycle chain oils. Details about lubricants can be found in their datasheets.

Except testing of lubricants in a standard way, Mogul grease was tested also in a way when only a thin film was applied on the gear. After it was applied, an excess grease was wiped with the swabs without using a cleaning solvent so only little amount remained on the surface. The gear drive was then warmed up like previously described.

One test was performed completely without a lubrication of the worm drive. Previous lubricant was cleaned even with more care to make sure anything remained. Then the smallest step test was performed immediately without running the warmup recipe. Another smallest step test was then performed after running the warmup recipe.

The move test and the smallest test was performed for each lubrication. Average values from the smallest step test results were calculated to make the comparison simple and clear. The comparison is depicted in following figures.

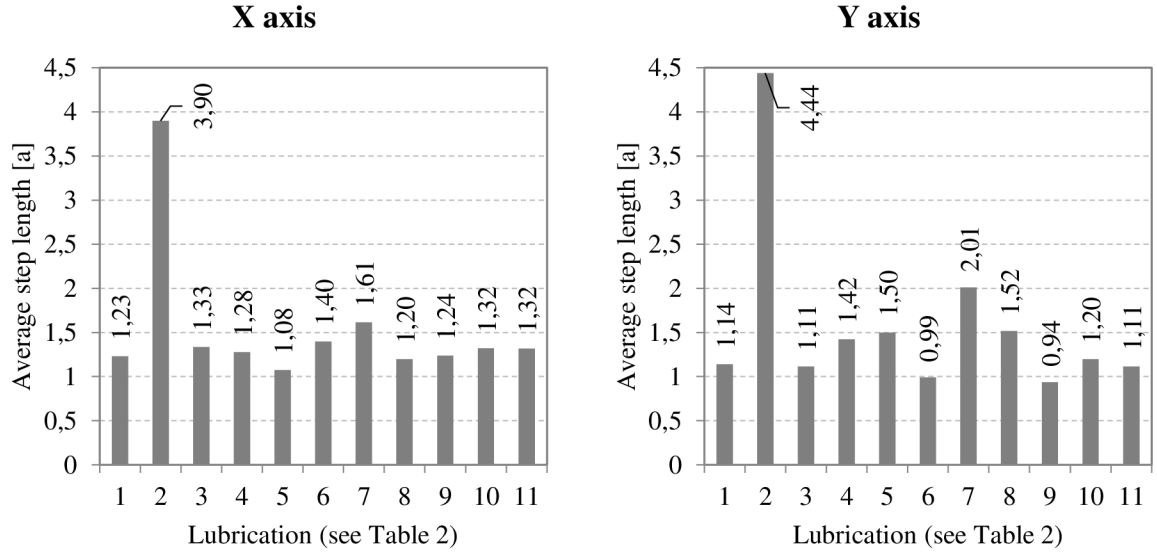

Figure 23: Average step length in relation to lubrication

Average step length varying in relation to lubrication is shown in the Figure 23. It is calculated from the whole smallest step test without considering movement direction. It means that if most steps were bigger in the positive direction and smaller in the negative direction then average value could lay near the desired $1a$ length. It is therefore important to consider standard deviation of step, which is shown in the Figure 24, again with relation to lubrication.

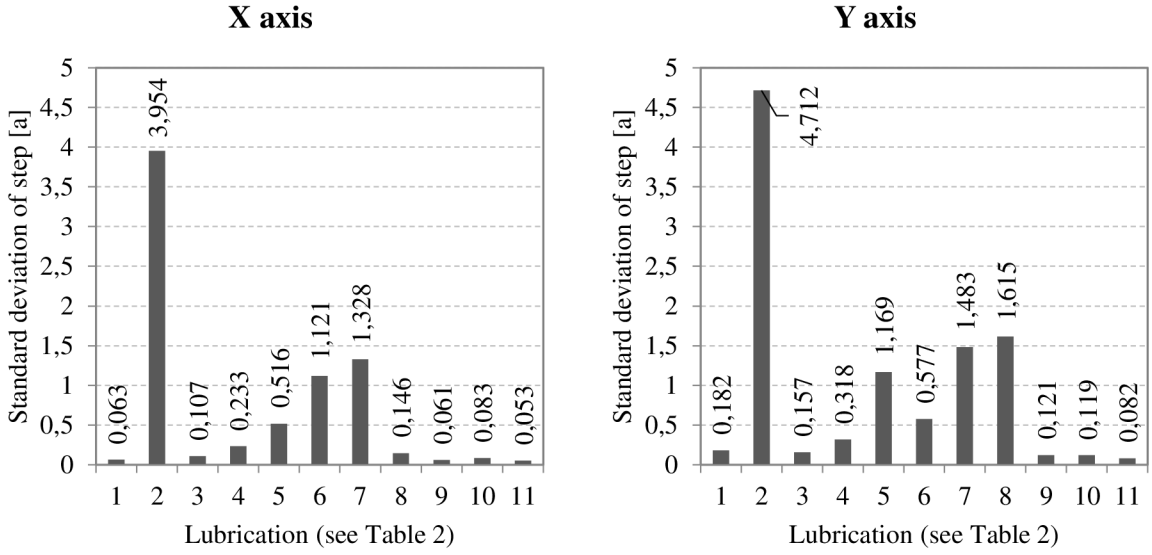

Figure 24: Standard deviation of step in relation to lubrication

If an average step length is very close to $1a$ but with high standard deviation, then the lubrication which lead to this result is useless. An example of high standard deviation is shown in the Figure 25. Aim is to find lubrication with average step as close to the desired length together with standard deviation as low as possible.

Not good results were achieved with the FeinOl oil. This oil has very low viscosity comparable to regular water. The worm drive without any lubrication was not working better either. On the other hand, good results were achieved with the Molykote, Renolit and Promicron greases all with high viscosity. These results were comparable to those achieved with currently used Braycote grease but they were not a lot better.

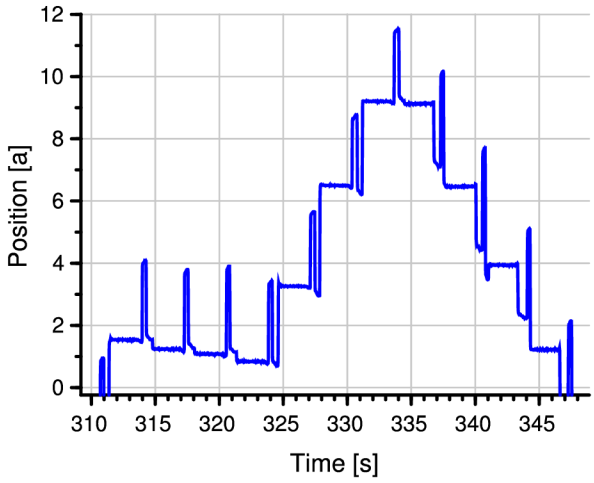

Figure 25: Example of high step deviation – Dry Lube in Y axis

Generally better results were achieved with higher viscosity lubricants – greases. No better than currently used Braycote greasing had been found. Therefore any change of lubrication of the worm drive is not suggested.

1.5. Pretension springs of the mechanism

The carriage of the mechanism is preloaded by two extension springs for each of X and Y axis. When the spring is mounted in the mechanism and the manipulator is in the middle of its range, the spring has length of $67.4\ mm$. When the nanomanipulator is moving, the length of the spring is changing only by $\pm 1\ mm$ what is limited by the range. Thanks to almost constant length, the pretension force exerted by the spring is also almost constant. The pretension force can be calculated from stiffness and prolongation of the spring. Currently the mechanism uses two $14\ N$ pretension springs T40826F for each axis, what makes a total pretension force of $28\ N$. For testing purposes, the force exerted by one spring is always stated. Total pretension force for an axis is then twice the force of a spring. The list of all tested springs is stated in the Table 3. [15]

Catalogue code	Manufacturer	Force at length of 67.4 mm
T40826F	Tevema	**14.0 N**
T40700G	Tevema	**6.2 N**
04_8_5	Hennlich	**4.0 N**
03_9_5	Hennlich	**2.3 N**
03_10_7	Hennlich	**1.6 N**
03_10_8	Hennlich	**1.0 N**

Table 3: Table of tested extension springs [16] [15]

The gravity of the nanomanipulator has to be considered since it can direct against the pretension force, which depends on the mounting position. At the standard mounting position, the Y axis is not influenced by the gravity because it is horizontal. Therefore all tests of various springs were performed for the Y axis only.

At the standard mounting position the force exerted by the gravity for X axis is equal $12.5\ N$, what was measured with force meter. A force exerted by springs then must be higher to be able to pre-load the mechanism. Having two springs of $14\ N$ minus the gravity gives the total pretension force of $15.5\ N$ for the X axis. If the $4\ N$ springs were mounted on the X axis, total $8\ N$ force would not overcome the gravity. That is another reason of testing springs only for the Y axis. After optimizing the springs for the Y axis, the suitable X axis springs then can be easily calculated by adding the gravity force to a desired total pretension force.

The move test and the smallest test was performed for each spring for the Y axis. The comparison of results is in the following Table 4. Since the $14\ N$ spring is currently used, the results of this spring are the same as stated in the 1.2.4 Current performance subhead and serve as comparison now.

14 N spring			
Position [a]	**Direction**	**Average [a]**	**Standard deviation [a]**
-4,00E+03	Positive	0,352	5,36E-02
-4,00E+03	Negative	1,360	1,33E-01
-2,00E+03	Positive	0,422	1,13E-01
-2,00E+03	Negative	1,382	1,43E-01
0,00E+00	Positive	0,362	5,44E-02
0,00E+00	Negative	1,468	1,12E-01
2,00E+03	Positive	0,324	1,22E-01
2,00E+03	Negative	1,398	2,22E-01
4,00E+03	Positive	0,890	1,45E-01
4,00E+03	Negative	1,406	1,08E-01

6.2 N spring			
Position [a]	**Direction**	**Average [a]**	**Standard deviation [a]**
-4,00E+03	Positive	0,878	4,86E-02
-4,00E+03	Negative	1,272	5,80E-02
-2,00E+03	Positive	1,010	4,36E-02
-2,00E+03	Negative	1,298	4,86E-02
0,00E+00	Positive	0,914	4,76E-02
0,00E+00	Negative	1,170	5,34E-02
2,00E+03	Positive	0,882	8,40E-02
2,00E+03	Negative	1,296	7,06E-02
4,00E+03	Positive	1,096	9,98E-02
4,00E+03	Negative	1,314	3,20E-02

4 N spring			
Position [a]	**Direction**	**Average [a]**	**Standard deviation [a]**
-4,00E+03	Positive	1,090	5,14E-02
-4,00E+03	Negative	1,194	2,70E-02
-2,00E+03	Positive	1,120	3,32E-02
-2,00E+03	Negative	1,234	4,76E-02
0,00E+00	Positive	1,112	4,72E-02
0,00E+00	Negative	1,212	3,12E-02
2,00E+03	Positive	1,066	1,18E-01
2,00E+03	Negative	1,218	5,06E-02
4,00E+03	Positive	1,154	8,94E-02
4,00E+03	Negative	1,262	3,50E-02

2.3 N spring			
Position [a]	**Direction**	**Average [a]**	**Standard deviation [a]**
-4,00E+03	Positive	1,076	6,22E-02
-4,00E+03	Negative	1,168	3,26E-02
-2,00E+03	Positive	1,112	7,72E-02
-2,00E+03	Negative	1,142	5,54E-02
0,00E+00	Positive	1,148	3,34E-02
0,00E+00	Negative	1,112	4,44E-02
2,00E+03	Positive	1,096	5,68E-02
2,00E+03	Negative	1,200	8,94E-02
4,00E+03	Positive	1,160	3,00E-02
4,00E+03	Negative	1,170	4,00E-02

1.6 N spring			
Position [a]	**Direction**	**Average [a]**	**Standard deviation [a]**
-4,00E+03	Positive	1,092	3,96E-02
-4,00E+03	Negative	1,126	3,70E-02
-2,00E+03	Positive	1,168	2,38E-02
-2,00E+03	Negative	1,116	2,78E-02
0,00E+00	Positive	1,102	3,34E-02
0,00E+00	Negative	1,074	2,96E-02
2,00E+03	Positive	1,148	1,92E-02
2,00E+03	Negative	1,150	5,00E-02
4,00E+03	Positive	1,190	2,54E-02
4,00E+03	Negative	1,126	4,04E-02

1 N spring			
Position [a]	**Direction**	**Average [a]**	**Standard deviation [a]**
-4,00E+03	Positive	1,012	3,12E-02
-4,00E+03	Negative	1,040	2,00E-02
-2,00E+03	Positive	1,060	2,54E-02
-2,00E+03	Negative	1,062	2,68E-02
0,00E+00	Positive	0,998	4,02E-02
0,00E+00	Negative	1,058	2,38E-02
2,00E+03	Positive	1,090	2,54E-02
2,00E+03	Negative	1,046	1,50E-02
4,00E+03	Positive	1,072	2,94E-02
4,00E+03	Negative	1,060	2,00E-02

Table 4: Smallest step test results for various springs (see Table 3)

Decreasing stiffness of the pretension springs results in better performance. Average step is closer to the desired $1a$ length with every decrease of the pretension force. Difference between the step length in positive and in negative direction is decreasing simultaneously together with decrease of standard deviation of the step length.

Average values from the smallest step test results were calculated to make the comparison simple and clear. The comparison is depicted in the following figure.

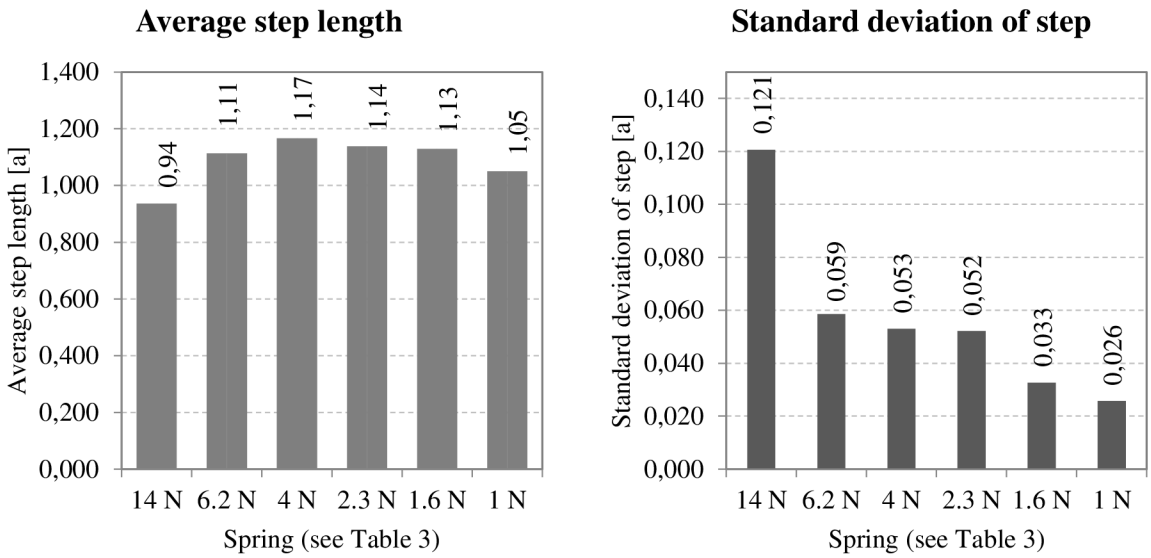

Figure 26: Comparison of various springs

Average step length and standard deviation of step are shown in the Figure 26. They are calculated from the whole smallest step test without considering movement direction similarly like it was explained in the previous subhead. The difference between positive and negative direction should be also considered when analyzing the average step length figure. The difference can be seen after closer view at the Table 4. The standard deviation shows significant decrease from the second tested spring. Then the decreasing continues but at lower rate. The best result were achieved with the 1 N spring, see also the Figure 27.

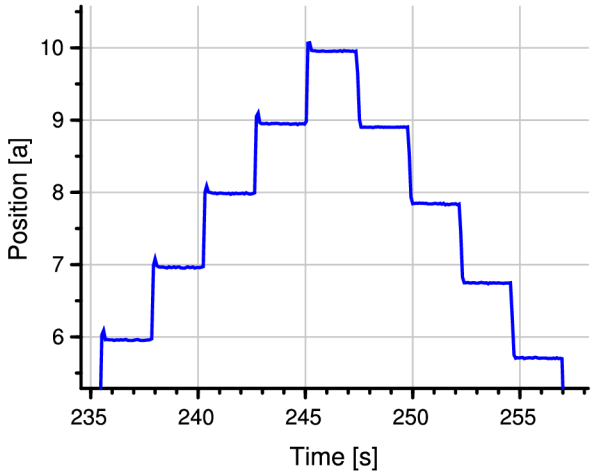

Figure 27: Best performance achieved with the 1 N spring

After considering the test results a change of springs was suggested. Despite the fact that the best results were achieved with the weakest $1\,N$ spring, the $4\,N$ spring results were chosen as sufficient in order to maintain the stiffness of the nanomanipulator. Then various mounting positions should be also considered before choosing an optimal pretension force.

1.6. Gear ratio of the worm drive

The angle of rotation of the DC motor is extremely small when performing the smallest step. Increase of the worm drive ratio will enlarge that angle. This could have an effect on the smallest performance.

Tested gear ratio is two times higher than currently used 40:1 which means 80:1. Increase of the worm drive ratio will decrease size of teeth of the gear what will decrease durability of the worm drive. This modification would be therefore applicable only if the pretension sprigs stiffness would be significantly reduced.

Figure 28: Comparison of gear modules (current on the right)

Testing of the gear ratio was done together with the testing of the pretension springs. It was done this way because currently used $14\,N$ pretension springs could overload new gear due to low module. Therefore the 80:1 gear drive was tested with $4\,N$ springs. It can be simply compared to the results of the 40:1 gear drive previously tested also with $4\,N$ springs. The test was performed for the Y axis.

40:1 gear ratio, 4 N spring			
Position [a]	**Direction**	**Average [a]**	**Standard deviation [a]**
-4,00E+03	Positive	1,090	5,14E-02
-4,00E+03	Negative	1,194	2,70E-02
-2,00E+03	Positive	1,120	3,32E-02
-2,00E+03	Negative	1,234	4,76E-02
0,00E+00	Positive	1,112	4,72E-02
0,00E+00	Negative	1,212	3,12E-02
2,00E+03	Positive	1,066	1,18E-01
2,00E+03	Negative	1,218	5,06E-02
4,00E+03	Positive	1,154	8,94E-02
4,00E+03	Negative	1,262	3,50E-02

80:1 gear ratio, 4 N spring			
Position [a]	**Direction**	**Average [a]**	**Standard deviation [a]**
-4,00E+03	Positive	1,122	4,02E-02
-4,00E+03	Negative	1,148	2,94E-02
-2,00E+03	Positive	1,138	2,68E-02
-2,00E+03	Negative	1,132	3,96E-02
0,00E+00	Positive	1,088	2,68E-02
0,00E+00	Negative	1,102	2,94E-02
2,00E+03	Positive	1,112	3,84E-02
2,00E+03	Negative	1,100	2,24E-02
4,00E+03	Positive	1,120	4,58E-02
4,00E+03	Negative	1,092	2,86E-02

Table 5: Smallest step test results for various gear ratios

Results of the smallest step test are shown in the Table 5. A close look will relieve a decrease of the standard deviation but additional analysis is needed for comparison of the gear ratio change results.

Average values from the smallest step test results were calculated and their comparison is depicted in the Figure 29. Average step length decreased only a little bit and so it could be considered to be the same as before. On the other hand the standard deviation of step dropped significantly, what confirms increased steadiness of the smallest step performance.

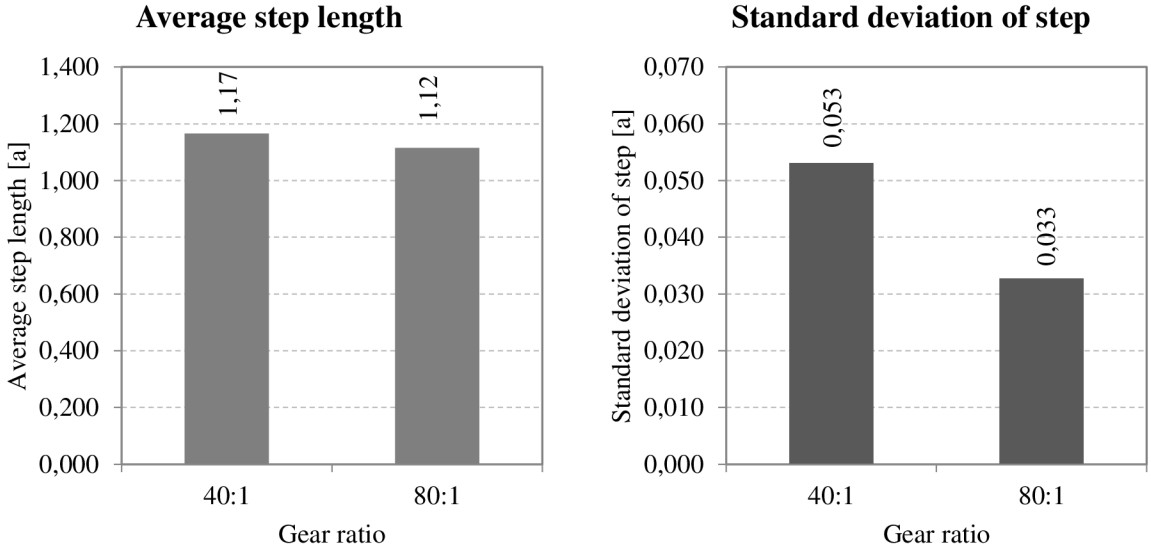

Figure 29: Comparison of various gear ratios

Increasing worm drive gear ratio results in better performance, but durability could be affected due to small gear module, what should be tested and verified before such change could be applied.

Because the change of the pretension spring was already confirmed to be sufficient and working, a further testing of increased worm drive ratio was not continued. FEI was satisfied with a simple change of the pretension springs and there was no need for any additional changes.

1.7. Final modification

Testing of lubrication of the worm drive, pretension spring stiffness and worm drive ratio was carried out. Results were analyzed and consulted with FEI. No better than currently used Braycote lubrication of the worm drive had been found. Change of pretension spring stiffness was suggested since the results confirmed an improvement. The worm drive ratio is not considered for a modification because the simple change of the pretension springs is sufficient.

As mentioned before, the nanomanipulator could be mounted in several different mounting positions. At each position the axes of the nanomanipulato are tilted so that the gravity influences the total pretension force. All possible mounting positions were considered and the pretension sprigs for each axis were calculated so that for every mounting position is the pretension force at least the sufficient $4\,N$. This resulted in the $4\,N$ springs for the Y axis and the $10.8\,N$ springs for the X axis. Influence of chosen springs to the total pretension force is shown in the Table 6.

	Before modification		**After modification**	
	Force of spring	**Total pretension force**	**Force of spring**	**Total pretension force**
X axis	14 N	28 N	10.8 N	9,1 N
Y axis	14 N	28 N	4 N	8 N

Table 6: Change of the pretension springs

After changing the pretension springs of the mechanism, the dynamic properties of the system slightly changed. Since the PID controller is tuned to a specific dynamic properties, additional tuning was required. This was done in the Control design application mentioned before. The data measured by the Xfer test was opened in the application which showed the Bode, Nyquist and Stability plots. The PID parameters were remained unchained to sustain the same speed of the controller. The modification shifted the resonance frequency of the system

what was simply corrected by changing the Lead Lag frequency. Additional filters designed to eliminate eventual notches were also set according to new shifted frequencies of the notches. The margins, which confirm whether the dynamic properties of the system meet the requirements, were also checked. The same procedure was done for both X and X axes.

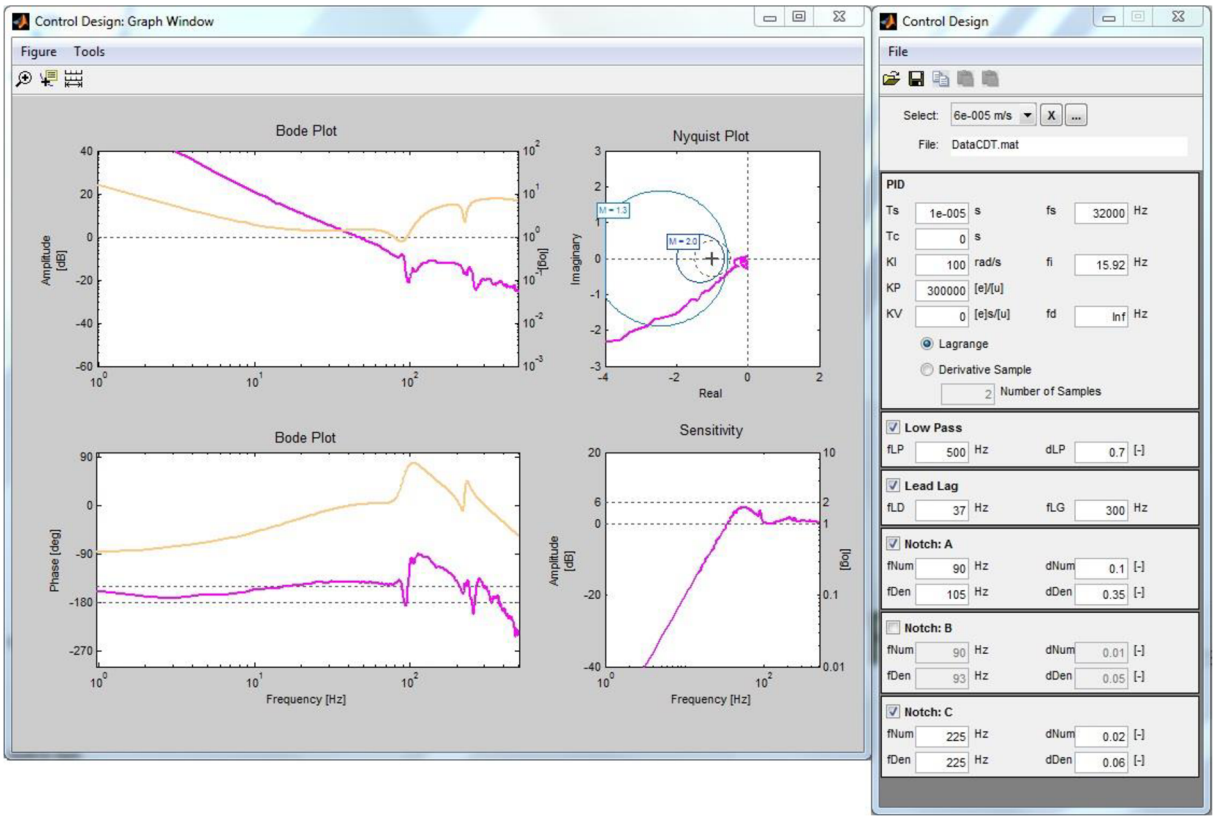

Figure 30: Control design application with modified parameters [11]

After suggesting the modification, a verification testing was carried out and is described together with results in the following last subhead of this chapter.

1.8. Performance after the modification

Performance after the modification measurement was done on five new microscopes equipped with new nanomanipulators. All tests were successful in meeting the requirements. Randomly picked results from one of the microscopes are shown and explained on the following pages. This results can be easily compared with the performance before modification in the subhead 1.2.4 on the page 29. Previously described test routines were performed for both axes as before. Starting with the move test in the Figure 31.

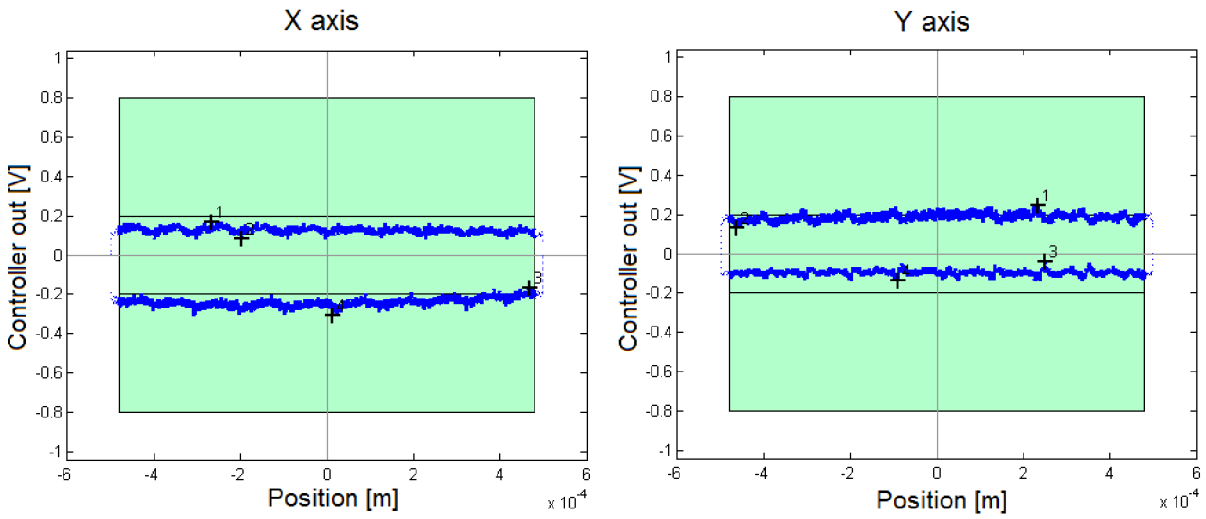

Figure 31: Move test [11]

The figure shows an increased smoothness of the operation for both axes thanks to the optimal pretension springs although the lubrication of the worm drive remained unchained. Comparing to the previous results, there is a decrease of the controller output voltage amplitude what means the DC motor is running easier. The difference between maximum and minimum value for each move is also lower what confirms movement stability. Now there is no significant difference between running of each axis as there was before.

The smallest step test was performed for both axes as before. A sample of typical performance during the test is shown in the Figure 32. The smallest step length for X axis in positive direction is a still bit bigger than desired $1a$ but less than before the modification. The back step in negative direction is also smaller. Precision of the Y axis is now much closer to the X axis. Any instabilities seen before were practically eliminated.

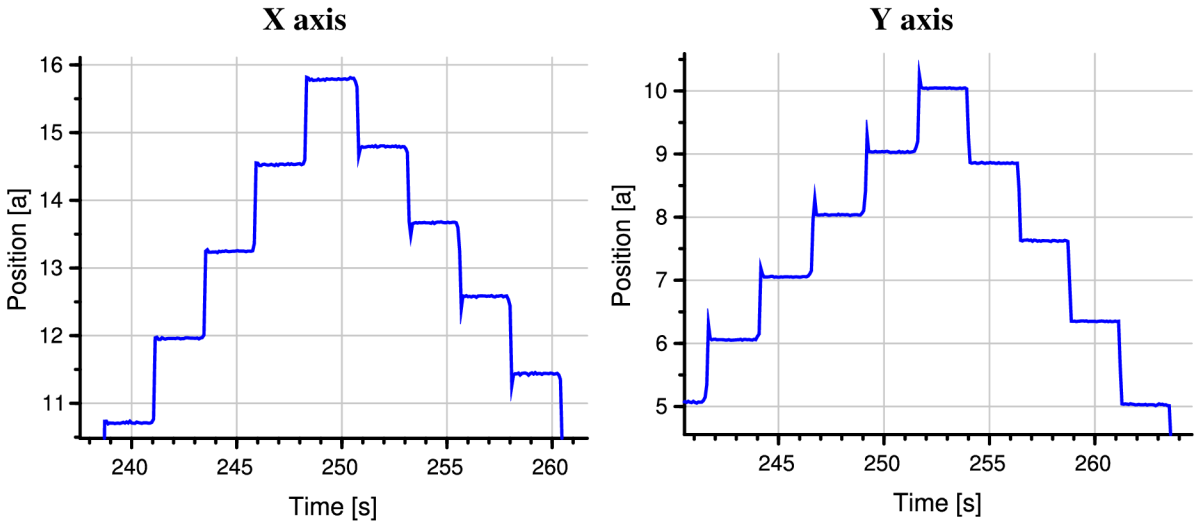

Figure 32: Typical smallest steps of X and Y axes

Complete results of the smallest step test are shown in the Table 7. The first column is a position of a set of steps. In comparison with the previous results the average step length is now much closer to desired length $1a$. There is also significant decrease of the standard deviation of step, especially for Y axis.

X axis				Y axis			
Position [a]	**Direction**	**Average [a]**	**Standard deviation [a]**	**Position [a]**	**Direction**	**Average [a]**	**Standard deviation [a]**
-4,00E+03	Positive	1,252	4,32E-02	-4,00E+03	Positive	1,100	2,74E-02
-4,00E+03	Negative	0,900	5,24E-02	-4,00E+03	Negative	1,226	2,96E-02
-2,00E+03	Positive	1,292	5,76E-02	-2,00E+03	Positive	0,994	4,16E-02
-2,00E+03	Negative	1,050	6,12E-02	-2,00E+03	Negative	1,240	2,54E-02
0,00E+00	Positive	1,282	4,82E-02	0,00E+00	Positive	1,002	2,48E-02
0,00E+00	Negative	1,060	8,16E-02	0,00E+00	Negative	1,256	2,70E-02
2,00E+03	Positive	1,272	2,94E-02	2,00E+03	Positive	0,968	6,94E-02
2,00E+03	Negative	1,060	4,64E-02	2,00E+03	Negative	1,258	4,26E-02
4,00E+03	Positive	1,244	3,12E-02	4,00E+03	Positive	0,982	2,38E-02
4,00E+03	Negative	1,114	5,50E-02	4,00E+03	Negative	1,258	2,86E-02

Table 7: Smallest step test results after modification

To make a simple comparison, average values from the table were calculated and plotted in the Figure 33 and the Figure 34. Closer the average step to desired length $1a$ the better. From these figures the improvement is now clearly visible. The Y axis is now performing in the same way as the X axis except the step is little bit longer in negative direction while for X axis it is

little bit longer in positive direction. It is because positive direction of the Y axis is directing against the pretension force while positive direction of the X axis is in direct of the pretension force.

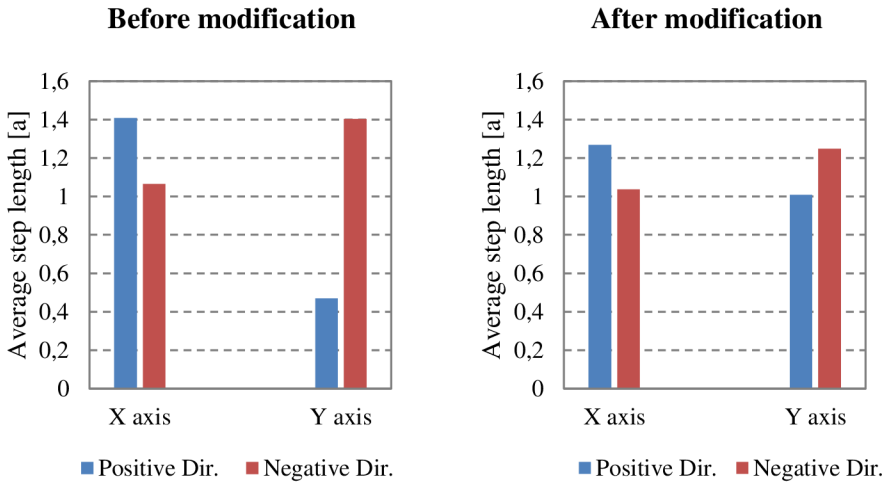

Figure 33: Average step length before and after modification

Increased precision of the nanomanipulator after modification is clearly visible in the following figure from the decrease of average standard deviation of step.

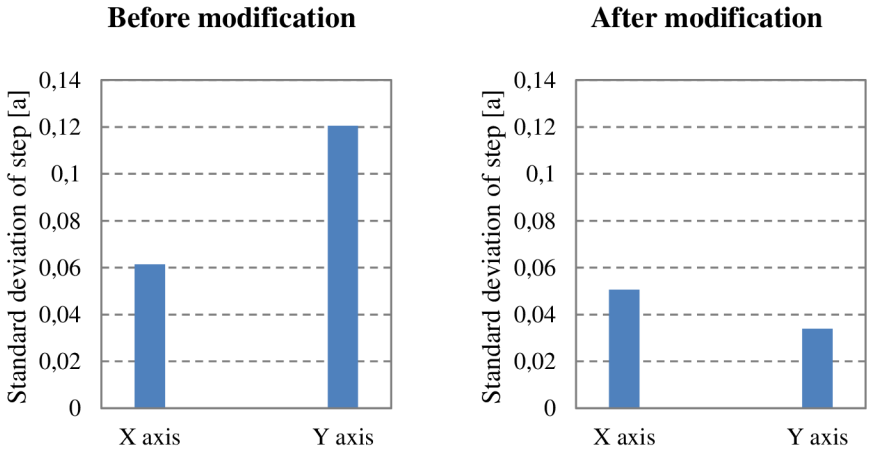

Figure 34: Average standard deviation of step before and after modification

The Xfer test was also performed for both axes as before. Results for the X axis are depicted in the Figure 35. Results for the Y axis are again very similar therefore not stated. After correct setting of the feedback control parameters, it is possible to say it was verified that the modification on the mechanism did not affected the dynamics of the nanomanipulator. The Xfer test confirms good dynamic properties of the system.

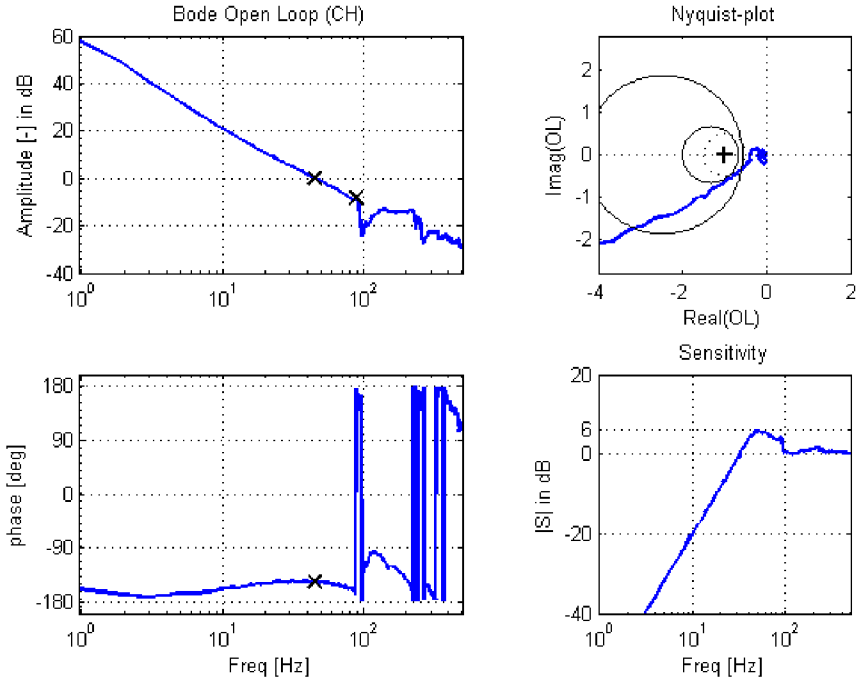

Figure 35: Xfer test for the X axis after the modification [11]

Overall result is increased precision of the smallest step together with increased steadiness of performing the smallest step. Smoother and easier running of the worm drive was also achieved in the line with the improvement, which could lead to higher durability.

Simple calculation was done to evaluate how great the improvement is. One whole smallest step test before and one after the modification was randomly picked. As reminder it is mentioned that 200 steps are performed in whole smallest step test in total. By calculation of average step length from the smallest step test before and after the modification for each axis and each moving directions it was possible to achieve total percentage of the improvement. Imprecision of the smallest step was decreased by 53.5 % if imprecision means how close is a performed step to its desired length. Standard deviation was also averaged for each axis. Average standard deviation of the smallest step was decreased by 44.7 %.

CONCLUSION

The purpose of this thesis was to improve the smallest step performance of the nanomanipulator used in electron microscope. It is possible to say that the main goal and also partial goals stated in the assignment were accomplished.

The overview part delivers a brief introduction to the role of the nanomanipulator in electron microscope, analyses the mechanics of the smallest step and searches for possible solutions to improvements.

Eight different lubricants of the worm gear have been tested and compared. The higher viscosity of a lubricant the better results when considering the smallest step performance. No better than the currently used Braycote greasing for the worm gear have been found. Weakening of pretension springs resulted in better performance and it has been chosen as real solution. Considering different mounting positions of the nanomanipulator, the optimal spring tension was calculated for both X and Y axes. Moreover one different worm drive gear ratio has been tested. Increasing the worm drive gear ratio resulted in better performance but durability could be affected due to small gear module. The worm drive gear ratio could be increased only if the pretension springs were significantly weakened. Mainly the change of the pretension springs was sufficient. Finally the parameters of feedback control were properly set in order to maintain the original dynamic properties of mechanism.

After considering test results, the weakening of the pretension springs together with the new parameters of the feedback control were chosen as modification while lubrication and gear ratio of the worm drive remains unchanged. Then, the new configuration have been fully tested on five brand new nanomanipulators to make sure the modification will not have any unwanted consequences. Result is the increase of the smallest step precision by 53.5 %.

Enhanced nanomanipulator is now in production. An all-out effort was put to make sure that the change will not deliver any negative effects in the future and will only bring extended possibilities.

BIBLIOGRAPHY

[1] FEI Company. *Introduction to electron microscopy*. 2010. ISBN 978 0 578 06276

[2] NOVÁK, Jakub. "FEI Scios Dualbeam" [Online]. Available: http:// www.novakjakub.cz/portfolio-item/fei-scios-dualbeam/. [Accessed 24 April 2016].

[3] FEI Company, "NanoManipulator Datasheet," 2013.

[4] Hyoung H. Kang, John F. King, Oliver D. Patterson, and Steven B. Herschbein, "High Volume and Fast Turnaround Automated Inline TEM Sample Preparation for Manufacturing Process Monitoring," in *ASM International*, 2010.

[5] FEI Company, "DualBeam TEM Sample Preparation Webcast," 2016. [Online]. Available: http://explore.fei.com/DualBeam-TEM-Sample-Preparation-Webcast. html. [Accessed 24 April 2016].

[6] FEI Company, *PDM, production system database,* 2016.

[7] Robert Munnig SCHMIDT, Georg SCHITTER a Jan van EIJ. *The design of high performance mechatronics, high-tech functionality by multidisciplinary system integration*. Amsterdam: Delft University Press, 2011, 753 p. ISBN 978-160-7508-267.

[8] Stuart T. SMITH, *Foundations of ultraprecision mechanism design.* Repr. with corr. Yverdon, Switzerland: Gordon and Breach Science Pub, 1994. ISBN 978-288-4490-016.

[9] PRECISION POINT, "Bode plot - Composition & interpretation," 2016.

[10] Robert H. Bishop, *The mechatronics Handbook*, Austin, Texas: The univesity of Texas at Austin, 2002.

[11] FEI Company, *TAD, testing software,* 2016.

[12] Rexroth Bosh Group, "Rexroth NYCe4000 Software manual," 2006.

[13] Bosch Rexroth Group, "Rexroth NYCe 4000 Excellence in motion control," 2008.

[14] Bosch Rexroth Group, "NYCe4000 API Reference Manual," 2009.

[15] Hennlich Industrietechnik, "Tažné pružiny, nerezová ocel," 2016.

[16] Tevema, "Extension springs," 2016.

LIST OF FIGURES

LIST OF TABLES